EUROPEAN ORGANIZATION FOR NUCLEAR RESEARCH

LEPEWWG/2001-01
ALEPH 2001-041PHYS 2001-015
DELPHI 2001-109 PHYS 897
L3 Note 2669
OPAL Technical Note TN 692
31st May 2001

A Combination of Preliminary Electroweak Measurements and Constraints on the Standard Model

The LEP Collaborations* ALEPH, DELPHI, L3, OPAL, the LEP Electroweak Working Group† and the SLD Heavy Flavour and Electroweak Groups‡

Prepared from Contributions of the LEP and SLD Experiments to the 2001 Winter Conferences.

Abstract

This note presents a combination of published and preliminary electroweak results from the four LEP collaborations and the SLD collaboration which were prepared for the 2001 winter conferences. Averages from Z resonance results are derived for hadronic and leptonic cross sections, the leptonic forward-backward asymmetries, the τ polarisation asymmetries, the $b\overline{b}$ and $c\overline{c}$ partial widths and forward-backward asymmetries and the $q\overline{q}$ charge asymmetry. Above the Z resonance, averages are derived for di–fermion cross sections and asymmetries, W–pair, Z–pair and single–W production cross section, electroweak gauge boson couplings, W mass and width and W decay branching ratios.

The main changes with respect to the experimental results presented in summer 2000 are updates to Z-pole heavy flavour results from SLD and LEP and the W mass from LEP. The results are compared with precise electroweak measurements from other experiments. Using a new evaluation of the hadronic vacuum polarisation, the parameters of the Standard Model are evaluated, first using the combined LEP electroweak measurements, and then using the full set of electroweak results.

*The LEP Collaborations each take responsibility for the preliminary results of their own.

†The members of the LEP Electroweak Working Group who contributed significantly to this note are : D. Abbaneo, J. Alcaraz, P. Antilogus, P. Bambade, E. Barberio, A. Blondel, S. Blyth, D. Bourilkov, R. Chierici, R. Clare, A. Ealet, M. Elsing, F. Fiedler, P. Garcia-Abia, M.W. Grünewald, J.B. Hansen, R. Hawkings, J. Holt, S. Jezequel, R.W.L. Jones, T. Kawamoto, N. Kjaer, M. Kobel, E. Lançon, W. Lohmann, C. Mariotti, M. Martinez, F. Matorras, C. Matteuzzi, E. Migliore, M.N. Minard, K. Mönig, M. Musy A. Olshevski, C. Parkes, U. Parzefall, Ch. Paus, M. Pepe-Altarelli, B. Pietrzyk, G. Quast, P. Renton, H. Rick, S. Riemann, J.M. Roney, K. Sachs, S. Spagnolo, A. Straessner, D. Strom, R. Tenchini, F. Teubert, E. Tournefier, H. Voss, C.P. Ward, N.K. Watson, St. Wynhoff.

‡N. de Groot, P.C. Rowson, D. Su.

1 Introduction

The four LEP experiments and SLD have recently presented [1] electroweak parameters using published and preliminary results. Results derived from the Z resonance are based on data recorded until the end of 1995 for the LEP experiments and 1998 for SLD. Since 1996 LEP has run at energies above the W-pair production threshold. In 2000, the final year of data taking at LEP, the delivered luminosity was as high as in 1999 while the centre-of-mass energy was increased close to 209 GeV.

LEP-I (1990-1995) Z-pole measurements are the hadronic and leptonic cross sections, the leptonic forward-backward asymmetries, the τ polarisation asymmetries, the $b\overline{b}$ and $c\overline{c}$ partial widths and forward-backward asymmetries and the $q\overline{q}$ charge asymmetry. The measurements of the left-right cross section asymmetry, the $b\overline{b}$ and $c\overline{c}$ partial widths and left-right-forward-backward asymmetries for b and c quarks from SLD are treated consistently with the LEP data. Many technical aspects of their combination are described in References 2, 3 and references therein.

The LEP-II (1996-2000) measurements are di–fermion cross sections and asymmetries; W–pair, Z–pair and single–W production cross sections, electroweak gauge boson couplings. W boson properties, like mass, width and decay branching ratios are also measured.

Several measurements included in the combinations are still preliminary.

This note is organised as follows:

Section 2 Z Line Shape and Leptonic Forward-Backward Asymmetries;

Section 3 τ Polarisation;

Section 4 Measurement of polarised asymmetries at SLD;

Section 5 Heavy Flavour Analyses;

Section 6 Inclusive Hadronic Charge Asymmetry;

Section 7 Fermion-Pair Production at Energies above the Z;

Section 8 W Boson Properties, including m_{W}, Branching Ratios, W–pair Production Cross Section;

Section 9 Single–W Production Cross Section;

Section 10 ZZ Production Cross Section;

Section 11 Electroweak Gauge Boson Couplings;

Section 12 Interpretation of the Results, Including the Combination of Results from LEP, SLD, Neutrino Interaction Experiments and from CDF and DØ;

Section 13 Prospects for the Future.

To allow a quick assessment, a box highlighting the updates is given at the beginning of each section.

2 Z Lineshape and Lepton Forward-Backward Asymmetries

Updates with respect to last summer:
Unchanged w.r.t. summer 2000: All experiments have updated their results, and all are now final. Recent theoretical developments have been included in the results and fits.

The results presented here are based on the full LEP-I data set. This includes the data taken during the energy scans in 1990 and 1991 in the range[1] $|\sqrt{s} - m_Z| < 3$ GeV, the data collected at the Z peak in 1992 and 1994 and the precise energy scans in 1993 and 1995 ($|\sqrt{s} - m_Z| < 1.8$ GeV). The total event statistics are given in Table 1. Details of the individual analyses can be found in References 4–7.

$q\overline{q}$					
year	A	D	L	O	all
'90/91	433	357	416	454	1660
'92	633	697	678	733	2741
'93	630	682	646	649	2607
'94	1640	1310	1359	1601	5910
'95	735	659	526	659	2579
total	4071	3705	3625	4096	15497

$\ell^+\ell^-$					
year	A	D	L	O	all
'90/91	53	36	39	58	186
'92	77	70	59	88	294
'93	78	75	64	79	296
'94	202	137	127	191	657
'95	90	66	54	81	291
total	500	384	343	497	1724

Table 1: The $q\overline{q}$ and $\ell^+\ell^-$ event statistics, in units of 10^3, used for the analysis of the Z line shape and lepton forward-backward asymmetries by the experiments ALEPH (A), DELPHI (D), L3 (L) and OPAL (O).

For the averaging of results the LEP experiments provide a standard set of 9 parameters describing the information contained in hadronic and leptonic cross sections and leptonic forward-backward asymmetries. These parameters are convenient for fitting and averaging since they have small correlations. They are:

- The mass and total width of the Z boson, where the definition is based on the Breit-Wigner denominator $(s - m_Z^2 + is\Gamma_Z/m_Z)$ with s-dependent width [8].
- The hadronic pole cross section of Z exchange:

$$\sigma_h^0 \equiv \frac{12\pi}{m_Z^2}\frac{\Gamma_{ee}\Gamma_{had}}{\Gamma_Z^2}. \tag{1}$$

  Here Γ_{ee} and Γ_{had} are the partial widths of the Z for decays into electrons and hadrons.
- The ratios:

$$R_e \equiv \Gamma_{had}/\Gamma_{ee}, \quad R_\mu \equiv \Gamma_{had}/\Gamma_{\mu\mu} \text{ and } R_\tau \equiv \Gamma_{had}/\Gamma_{\tau\tau}. \tag{2}$$

  Here $\Gamma_{\mu\mu}$ and $\Gamma_{\tau\tau}$ are the partial widths of the Z for the decays $Z \to \mu^+\mu^-$ and $Z \to \tau^+\tau^-$. Due to the mass of the τ lepton, a difference of 0.2% is expected between the values for R_e and R_μ, and the value for R_τ, even under the assumption of lepton universality [9].
- The pole asymmetries, $A_{FB}^{0,e}$, $A_{FB}^{0,\mu}$ and $A_{FB}^{0,\tau}$, for the processes $e^+e^- \to e^+e^-$, $e^+e^- \to \mu^+\mu^-$ and $e^+e^- \to \tau^+\tau^-$. In terms of the real parts of the effective vector and axial-vector neutral current couplings of fermions, g_{Vf} and g_{Af}, the pole asymmetries are expressed as

$$A_{FB}^{0,f} \equiv \frac{3}{4}\mathcal{A}_e\mathcal{A}_f \tag{3}$$

  with

$$\mathcal{A}_f \equiv \frac{2g_{Vf}g_{Af}}{g_{Vf}^2 + g_{Af}^2} = 2\frac{g_{Vf}/g_{Af}}{1 + (g_{Vf}/g_{Af})^2}. \tag{4}$$

[1] In this note $\hbar = c = 1$.

The imaginary parts of the vector and axial-vector coupling constants as well as real and imaginary parts of the photon vacuum polarisation are taken into account explicitly in the fitting formulae and are fixed to their Standard Model values. The fitting procedure takes into account the effects of initial-state radiation [8] to $\mathcal{O}(\alpha^3)$ [10–12], as well as the t-channel and the s-t interference contributions in the case of e^+e^- final states.

The set of 9 parameters does not describe hadron and lepton-pair production completely, because it does not include the interference of the s-channel Z exchange with the s-channel γ exchange. For the results presented in this section and used in the rest of the note, the γ-exchange contributions and the hadronic γZ interference terms are fixed to their Standard Model values. The leptonic γZ interference terms are expressed in terms of the effective couplings.

The four sets of 9 parameters provided by the LEP experiments are presented in Table 2. For performing the average over these four sets of nine parameters, the overall covariance matrix is constructed from the covariance matrices of the individual LEP experiments and common systematic errors [2]. The common systematic errors include theoretical errors as well as errors arising from the uncertainty in the LEP beam energy. The beam energy uncertainty contributes an uncertainty of ±1.7 MeV to m_Z and ±1.2 MeV to Γ_Z. In addition, the uncertainty in the centre-of-mass energy spread of about ±1 MeV contributes ±0.2 MeV to Γ_Z. The theoretical error on calculations of the small-angle Bhabha cross section is ±0.054 % [13] for OPAL and ±0.061 % [14] for all other experiments, and results in the largest common systematic uncertainty on σ_h^0. QED radiation, dominated by photon radiation from the initial state electrons, contributes a common uncertainty of ±0.02 % on σ_h^0, of ±0.3 MeV on m_Z and of ±0.2 MeV on Γ_Z. The contribution of t-channel diagrams and the s-t interference in $Z \to e^+e^-$ leads to an additional theoretical uncertainty estimated to be ±0.24 on R_e and ±0.0014 on $A_{FB}^{0,e}$, which are fully anti–correlated. Uncertainties from the model-independent parameterisation of the energy dependence of the cross section are almost negligible, if the definitions of Reference [15] are applied. Through unavoidable Standard Model remnants, dominated by the need to fix the γ-Z interference contribution in the $q\overline{q}$ channel, there is some small dependence of ±0.2 MeV of m_Z on the Higgs mass, m_H (in the range 100 GeV to 1000 GeV) and the value of the electromagnetic coupling constant. Such "parametric" errors are negligible for the other pseudo-observables. The combined parameter set and its correlation matrix are given in Table 3.

If lepton universality is assumed, the set of 9 parameters is reduced to a set of 5 parameters. R_ℓ is defined as $R_\ell \equiv \Gamma_{had}/\Gamma_{\ell\ell}$, where $\Gamma_{\ell\ell}$ refers to the partial Z width for the decay into a pair of massless charged leptons. The data of each of the four LEP experiments are consistent with lepton universality (the difference in χ^2 over the difference in d.o.f. with and without the assumption of lepton universality is 3/4, 6/4, 5/4 and 3/4 for ALEPH, DELPHI, L3 and OPAL, respectively). The lower part of Table 3 gives the combined result and the corresponding correlation matrix. Figure 1 shows, for each lepton species and for the combination assuming lepton universality, the resulting 68% probability contours in the R_ℓ-$A_{FB}^{0,\ell}$ plane. Good agreement is observed.

For completeness the partial decay widths of the Z boson are listed in Table 4, although they are

		correlations								
		m_Z	Γ_Z	σ_h^0	R_e	R_μ	R_τ	$A_{FB}^{0,e}$	$A_{FB}^{0,\mu}$	$A_{FB}^{0,\tau}$
χ^2/N_{df} = 169/176					ALEPH					
m_Z [GeV]	91.1891 ± 0.0031	1.00								
Γ_Z [GeV]	2.4959 ± 0.0043	.038	1.00							
σ_h^0 [nb]	41.558 ± 0.057	−.091	−.383	1.00						
R_e	20.690 ± 0.075	.102	.004	.134	1.00					
R_μ	20.801 ± 0.056	−.003	.012	.167	.083	1.00				
R_τ	20.708 ± 0.062	−.003	.004	.152	.067	.093	1.00			
$A_{FB}^{0,e}$	0.0184 ± 0.0034	−.047	.000	−.003	−.388	.000	.000	1.00		
$A_{FB}^{0,\mu}$	0.0172 ± 0.0024	.072	.002	.002	.019	.013	.000	−.008	1.00	
$A_{FB}^{0,\tau}$	0.0170 ± 0.0028	.061	.002	.002	.017	.000	.011	−.007	.016	1.00
χ^2/N_{df} = 177/168					DELPHI					
m_Z [GeV]	91.1864 ± 0.0028	1.00								
Γ_Z [GeV]	2.4876 ± 0.0041	.047	1.00							
σ_h^0 [nb]	41.578 ± 0.069	−.070	−.270	1.00						
R_e	20.88 ± 0.12	.063	.000	.120	1.00					
R_μ	20.650 ± 0.076	−.003	−.007	.191	.054	1.00				
R_τ	20.84 ± 0.13	.001	−.001	.113	.033	.051	1.00			
$A_{FB}^{0,e}$	0.0171 ± 0.0049	.057	.001	−.006	−.106	.000	−.001	1.00		
$A_{FB}^{0,\mu}$	0.0165 ± 0.0025	.064	.006	−.002	.025	.008	.000	−.016	1.00	
$A_{FB}^{0,\tau}$	0.0241 ± 0.0037	.043	.003	−.002	.015	.000	.012	−.015	.014	1.00
χ^2/N_{df} = 158/166					L3					
m_Z [GeV]	91.1897 ± 0.0030	1.00								
Γ_Z [GeV]	2.5025 ± 0.0041	.065	1.00							
σ_h^0 [nb]	41.535 ± 0.054	.009	−.343	1.00						
R_e	20.815 ± 0.089	.108	−.007	.075	1.00					
R_μ	20.861 ± 0.097	−.001	.002	.077	.030	1.00				
R_τ	20.79 ± 0.13	.002	.005	.053	.024	.020	1.00			
$A_{FB}^{0,e}$	0.0107 ± 0.0058	−.045	.055	−.006	−.146	−.001	−.003	1.00		
$A_{FB}^{0,\mu}$	0.0188 ± 0.0033	.052	.004	.005	.017	.005	.000	.011	1.00	
$A_{FB}^{0,\tau}$	0.0260 ± 0.0047	.034	.004	.003	.012	.000	.007	−.008	.006	1.00
χ^2/N_{df} = 155/194					OPAL					
m_Z [GeV]	91.1858 ± 0.0030	1.00								
Γ_Z [GeV]	2.4948 ± 0.0041	.049	1.00							
σ_h^0 [nb]	41.501 ± 0.055	.031	−.352	1.00						
R_e	20.901 ± 0.084	.108	.011	.155	1.00					
R_μ	20.811 ± 0.058	.001	.020	.222	.093	1.00				
R_τ	20.832 ± 0.091	.001	.013	.137	.039	.051	1.00			
$A_{FB}^{0,e}$	0.0089 ± 0.0045	−.053	−.005	.011	−.222	−.001	.005	1.00		
$A_{FB}^{0,\mu}$	0.0159 ± 0.0023	.077	−.002	.011	.031	.018	.004	−.012	1.00	
$A_{FB}^{0,\tau}$	0.0145 ± 0.0030	.059	−.003	.003	.015	−.010	.007	−.010	.013	1.00

Table 2: Line Shape and asymmetry parameters from fits to the data of the four LEP experiments and their correlation coefficients.

more correlated than the ratios given in Table 3. The leptonic pole cross-section, σ_ℓ^0, defined as

$$\sigma_\ell^0 \equiv \frac{12\pi}{m_Z^2}\frac{\Gamma_{\ell\ell}^2}{\Gamma_Z^2},$$

in analogy to σ_h^0, is shown in the last line of the Table. Because QCD final state corrections appear quadratically in the denominator via Γ_Z, σ_ℓ^0 has a higher sensitivity to α_s than σ_h^0 or R_ℓ, where the

dependence on QCD corrections is only linear.

without lepton universality		correlations								
χ^2/N_{df} = 32.6/27		m_Z	Γ_Z	σ_h^0	R_e	R_μ	R_τ	$A_{FB}^{0,e}$	$A_{FB}^{0,\mu}$	$A_{FB}^{0,\tau}$
m_Z [GeV]	91.1876± 0.0021	1.00								
Γ_Z [GeV]	2.4952 ± 0.0023	−.024	1.00							
σ_h^0 [nb]	41.541 ± 0.037	−.044	−.297	1.00						
R_e	20.804 ± 0.050	.078	−.011	.105	1.00					
R_μ	20.785 ± 0.033	.000	.008	.131	.069	1.00				
R_τ	20.764 ± 0.045	.002	.006	.092	.046	.069	1.00			
$A_{FB}^{0,e}$	0.0145 ± 0.0025	−.014	.007	.001	−.371	.001	.003	1.00		
$A_{FB}^{0,\mu}$	0.0169 ± 0.0013	.046	.002	.003	.020	.012	.001	−.024	1.00	
$A_{FB}^{0,\tau}$	0.0188 ± 0.0017	.035	.001	.002	.013	−.003	.009	−.020	.046	1.00
with lepton universality										
χ^2/N_{df} = 36.5/31		m_Z	Γ_Z	σ_h^0	R_ℓ	$A_{FB}^{0,\ell}$				
m_Z [GeV]	91.1875± 0.0021	1.00								
Γ_Z [GeV]	2.4952 ± 0.0023	−.023	1.00							
σ_h^0 [nb]	41.540 ± 0.037	−.045	−.297	1.00						
R_ℓ	20.767 ± 0.025	.033	.004	.183	1.00					
$A_{FB}^{0,\ell}$	0.0171 ± 0.0010	.055	.003	.006	−.056	1.00				

Table 3: Average line shape and asymmetry parameters from the data of the four LEP experiments, without and with the assumption of lepton universality.

without lepton universality		correlations			
Γ_{had} [MeV]	1745.8 ±2.7	1.00			
Γ_{ee} [MeV]	83.92±0.12	−0.29	1.00		
$\Gamma_{\mu\mu}$ [MeV]	83.99±0.18	0.66	−0.20	1.00	
$\Gamma_{\tau\tau}$ [MeV]	84.08±0.22	0.54	−0.17	0.39	1.00
with lepton universality					
Γ_{inv} [MeV]	499.0 ±1.5	1.00			
Γ_{had} [MeV]	1744.4 ±2.0	−0.29	1.00		
$\Gamma_{\ell\ell}$ [MeV]	83.984±0.086	0.49	0.39	1.00	
$\Gamma_{inv}/\Gamma_{\ell\ell}$	5.942 ±0.016				
σ_ℓ^0 [nb]	2.0003±0.0027				

Table 4: Partial decay widths of the Z boson, derived from the results of the 9-parameter averages in Table 3. In the case of lepton universality, $\Gamma_{\ell\ell}$ refers to the partial Z width for the decay into a pair of massless charged leptons.

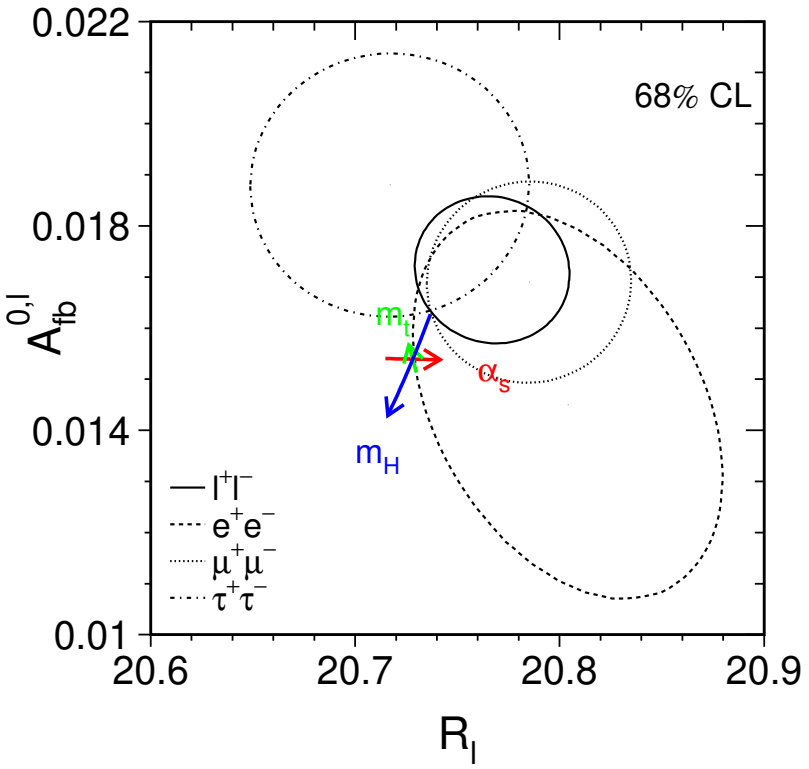

Figure 1: Contours of 68% probability in the R_ℓ-$A_{\rm FB}^{0,\ell}$ plane. For better comparison the results for the τ lepton are corrected to correspond to the massless case. The Standard Model prediction for $m_{\rm Z} = 91.1875$ GeV, $m_{\rm t} = 174.3$ GeV, $m_{\rm H} = 300$ GeV, and $\alpha_{\rm s}(m_{\rm Z}^2) = 0.119$ is also shown. The lines with arrows correspond to the variation of the Standard Model prediction when $m_{\rm t}$, $m_{\rm H}$ and $\alpha_{\rm s}(m_{\rm Z}^2)$ are varied in the intervals $m_{\rm t} = 174.3 \pm 5.1$ GeV, $m_{\rm H} = 300^{+700}_{-187}$ GeV, and $\alpha_{\rm s}(m_{\rm Z}^2) = 0.119 \pm 0.002$, respectively. The arrows point in the direction of increasing values of $m_{\rm t}$, $m_{\rm H}$ and $\alpha_{\rm s}$.

3 The τ Polarisation

Updates with respect to last summer:
OPAL have finalised their results. While all results are now final, the combination procedure itself is still preliminary.

The longitudinal τ polarisation $\mathcal{P}_\tau$ of τ pairs produced in Z decays is defined as

$$\mathcal{P}_\tau \equiv \frac{\sigma_{\rm R} - \sigma_{\rm L}}{\sigma_{\rm R} + \sigma_{\rm L}}, \tag{5}$$

where $\sigma_{\rm R}$ and $\sigma_{\rm L}$ are the τ-pair cross sections for the production of a right-handed and left-handed τ^-, respectively. The distribution of $\mathcal{P}_\tau$ as a function of the polar scattering angle θ between the e^- and the τ^-, at $\sqrt{s} = m_{\rm Z}$, is given by

$$\mathcal{P}_\tau(\cos\theta) = -\frac{\mathcal{A}_\tau(1+\cos^2\theta) + 2\mathcal{A}_{\rm e}\cos\theta}{1+\cos^2\theta + 2\mathcal{A}_\tau\mathcal{A}_{\rm e}\cos\theta}, \tag{6}$$

with $\mathcal{A}_{\rm e}$ and $\mathcal{A}_\tau$ as defined in Equation (4). Equation (6) is valid for pure Z exchange. The effects of γ exchange, γ-Z interference and electromagnetic radiative corrections in the initial and final states are taken into account in the experimental analyses. In particular, these corrections account for the $\sqrt{s}$ dependence of the τ polarisation, which is important because the off-peak data are included in the event samples for all experiments. When averaged over all production angles $\mathcal{P}_\tau$ is a measurement of $\mathcal{A}_\tau$. As a function of $\cos\theta$, $\mathcal{P}_\tau(\cos\theta)$ provides nearly independent determinations of both $\mathcal{A}_\tau$ and $\mathcal{A}_{\rm e}$, thus allowing a test of the universality of the couplings of the Z to e and τ.

Each experiment makes separate $\mathcal{P}_\tau$ measurements using the five τ decay modes $e\nu\overline{\nu}$, $\mu\nu\overline{\nu}$, $\pi\nu$, $\rho\nu$ and $a_1\nu$ [16–19]. The $\rho\nu$ and $\pi\nu$ are the most sensitive channels, contributing weights of about 40% each in the average. DELPHI and L3 have also used an inclusive hadronic analysis. The combination is made using the results from each experiment already averaged over the τ decay modes.

3.1 Results

Tables 5 and 6 show the most recent results for $\mathcal{A}_\tau$ and $\mathcal{A}_{\rm e}$ obtained by the four LEP collaborations [16–19] and their combination. Common systematic errors arise from uncertainties in the decay radiation in the $\pi\nu$ and $\rho\nu$ channels, and in the modelling of the a_1 decays [20]. These errors and their correlations need further investigation and will be taken into account for the final combination (see Reference 18). For the current combination the systematic errors on $\mathcal{A}_\tau$ and $\mathcal{A}_{\rm e}$ are treated as uncorrelated between the experiments. The statistical correlation between the extracted values of $\mathcal{A}_\tau$ and $\mathcal{A}_{\rm e}$ is small ($\leq$ 5%), and is neglected.

The average values for $\mathcal{A}_\tau$ and $\mathcal{A}_{\rm e}$:

$$\mathcal{A}_\tau = 0.1439 \pm 0.0042 \tag{7}$$
$$\mathcal{A}_{\rm e} = 0.1498 \pm 0.0048\,, \tag{8}$$

are compatible, in agreement with lepton universality. Assuming e-τ universality, the values for $\mathcal{A}_\tau$ and $\mathcal{A}_{\rm e}$ can be combined. This combination is performed neglecting any possible common systematic error between $\mathcal{A}_\tau$ and $\mathcal{A}_{\rm e}$ within a given experiment, as these errors are also estimated to be small. The combined result of $\mathcal{A}_\tau$ and $\mathcal{A}_{\rm e}$ is:

$$\mathcal{A}_\ell = 0.1464 \pm 0.0032\,. \tag{9}$$

Experiment		$\mathcal{A}_\tau$
ALEPH	(90 - 95), final	$0.1451 \pm 0.0052 \pm 0.0029$
DELPHI	(90 - 95), final	$0.1359 \pm 0.0079 \pm 0.0055$
L3	(90 - 95), final	$0.1476 \pm 0.0088 \pm 0.0062$
OPAL	(90 - 95), final	$0.1456 \pm 0.0076 \pm 0.0057$
LEP Average	preliminary	0.1439 ± 0.0041

Table 5: LEP results for $\mathcal{A}_\tau$. The χ^2/d.o.f. for the average is 0.9/3. The first error is statistical and the second systematic. In the LEP average, statistical and systematic errors are combined in quadrature. The systematic component of the error is ± 0.0022.

Experiment		$\mathcal{A}_e$
ALEPH	(90 - 95), final	$0.1504 \pm 0.0068 \pm 0.0008$
DELPHI	(90 - 95), final	$0.1382 \pm 0.0116 \pm 0.0005$
L3	(90 - 95), final	$0.1678 \pm 0.0127 \pm 0.0030$
OPAL	(90 - 95), final	$0.1454 \pm 0.0108 \pm 0.0036$
LEP Average	preliminary	0.1498 ± 0.0048

Table 6: LEP results for $\mathcal{A}_e$. The χ^2/d.o.f. for the average is 3.1/3. The first error is statistical and the second systematic. In the LEP average, statistical and systematic errors are combined in quadrature. The systematic component of the error is ± 0.0008.

4 Measurement of A_{LR} at SLC

Updates with respect to last summer:
Unchanged w.r.t. summer 2000: SLD have final results for A_{LR} and the leptonic left-right forward-backward asymmetries.

The measurement of the left-right cross section asymmetry (A_{LR}) by SLD [21] at the SLC provides a systematically precise, statistics-dominated determination of the coupling $\mathcal{A}_e$, and is presently the most precise single measurement, with the smallest systematic error, of this quantity. In principle the analysis is straightforward: one counts the numbers of Z bosons produced by left and right longitudinally polarised electrons, forms an asymmetry, and then divides by the luminosity-weighted e^- beam polarisation magnitude (the e^+ beam is not polarised):

$$A_{LR} = \frac{N_L - N_R}{N_L + N_R} \frac{1}{P_e}. \quad (10)$$

Since the advent of high polarisation "strained lattice" GaAs photocathodes (1994), the average electron polarisation at the interaction point has been in the range 73% to 77%. The method requires no detailed final state event identification (e^+e^- final state events are removed, as are non-Z backgrounds) and is insensitive to all acceptance and efficiency effects. The small total systematic error of 0.64% is dominated by the 0.50% systematic error in the determination of the e^- polarisation. The statistical error on A_{LR} is about 1.3%.

The precision Compton polarimeter detects beam electrons that have been scattered by photons from a circularly polarised laser. Two additional polarimeters that are sensitive to the Compton-scattered photons and which are operated in the absence of positron beam, have verified the precision polarimeter result and are used to set a calibration uncertainty of 0.4%. In 1998, a dedicated experiment was performed in order to directly test the expectation that accidental polarisation of the positron beam was negligible; the e^+ polarisation was found to be consistent with zero (-0.02 ± 0.07)%.

The A_{LR} analysis includes several very small corrections. The polarimeter result is corrected for higher order QED and accelerator related effects, a total of (-0.22 ± 0.15)% for 1997/98 data. The event asymmetry is corrected for backgrounds and accelerator asymmetries, a total of $(+0.15 \pm 0.07)$%, for 1997/98 data.

The translation of the A_{LR} result to a "pole" value is a (-2.5 ± 0.4)% effect, where the uncertainty arises from the precision of the centre-of-mass energy determination. This small error due to the beam energy measurement is slightly larger than seen previously (it was closer to 0.3%) and reflects the results of a scan of the Z peak used to calibrate the energy spectrometers to m_Z from LEP data, which was performed for the first time during the most recent SLC run. The pole value, A^0_{LR}, is equivalent to a measurement of $\mathcal{A}_e$.

The 2000 result is included in a running average of all of the SLD A_{LR} measurements (1992, 1993, 1994/1995, 1996, 1997 and 1998). This updated result for A^0_{LR} ($\mathcal{A}_e$) is 0.1514 ± 0.0022. In addition, the left-right forward-backward asymmetries for leptonic final states are measured [22]. From these, the parameters $\mathcal{A}_e$, $\mathcal{A}_\mu$ and $\mathcal{A}_\tau$ can be determined. The results are $\mathcal{A}_e = 0.1544 \pm 0.0060$, $\mathcal{A}_\mu = 0.142 \pm 0.015$ and $\mathcal{A}_\tau = 0.136 \pm 0.015$. The lepton-based result for $\mathcal{A}_e$ can be combined with the A^0_{LR} result to yield $\mathcal{A}_e = 0.1516 \pm 0.0021$, including small correlations in the systematic errors. The correlation of this measurement with $\mathcal{A}_\mu$ and $\mathcal{A}_\tau$ is indicated in Table 7.

Assuming lepton universality, the A_{LR} result and the results on the leptonic left-right forward-backward asymmetries can be combined, while accounting for small correlated systematic errors,

yielding

$$\mathcal{A}_\ell = 0.1513 \pm 0.0021. \tag{11}$$

	$\mathcal{A}_e$	$\mathcal{A}_\mu$	$\mathcal{A}_\tau$
$\mathcal{A}_e$	1.000		
$\mathcal{A}_\mu$	0.038	1.000	
$\mathcal{A}_\tau$	0.033	0.007	1.000

Table 7: Correlation coefficients between $\mathcal{A}_e$, $\mathcal{A}_\mu$ and $\mathcal{A}_\tau$

5 Results from b and c Quarks

Updates with respect to last summer:
ALEPH has updated their $A_{FB}^{b\bar{b}}$ jetcharge measurement using a neural net charge tag
DELPHI has presented new measurements of $A_{FB}^{b\bar{b}}$ using a neural net charge tag
SLD has $R_c$and most $\mathcal{A}_b$ and $\mathcal{A}_c$ measurements.

The relevant quantities in the heavy quark sector at LEP/SLD which are currently determined by the combination procedure are:

- The ratios of the b and c quark partial widths of the Z to its total hadronic partial width: $R_b^0 \equiv \Gamma_{b\bar{b}}/\Gamma_{had}$ and $R_c^0 \equiv \Gamma_{c\bar{c}}/\Gamma_{had}$.
- The forward-backward asymmetries, $A_{FB}^{b\bar{b}}$ and $A_{FB}^{c\bar{c}}$.
- The final state coupling parameters $\mathcal{A}_b$, $\mathcal{A}_c$ obtained from the left-right-forward-backward asymmetry at SLD.
- The semileptonic branching ratios, BR($b \to \ell$), BR($b \to c \to \bar{\ell}$) and BR($c \to \ell$), and the average time-integrated $B^0\overline{B^0}$ mixing parameter, $\overline{\chi}$. These are often determined at the same time or with similar methods as the asymmetries. Including them in the combination greatly reduces the errors. For example the measurements of $\overline{\chi}$ act as an effective measurement of the charge tagging efficiency, so that all errors coming from the mixture of different lepton sources in $b\overline{b}$ events cancel in the asymmetries.
- The probability that a c quark produces a D^+, D_s, D^{*+} meson[2] or a charmed baryon. The probability that a c quark fragments into a D^0 is calculated from the constraint that the probabilities for the weakly decaying charmed hadrons add up to one.

A full description of the averaging procedure is published in [3]; the main motivations for the procedure are outlined here. Several analyses measure more than one parameter simultaneously, for example the asymmetry measurements with leptons or D mesons. Some of the measurements of electroweak parameters depend explicitly on the values of other parameters, for example R_b depends on R_c. The common tagging and analysis techniques lead to common sources of systematic uncertainty, in particular for the double-tag measurements of R_b. The starting point for the combination is to ensure that all the analyses use a common set of assumptions for input parameters which give rise to systematic uncertainties. The input parameters are updated and extended [23,24] to accommodate new analyses and more recent measurements. The correlations and interdependences of the input measurements are then taken into account in a χ^2 minimisation which results in the combined electroweak parameters and their correlation matrix.

In a first fit the asymmetry measurements on peak, above peak and below peak are corrected to three common centre-of-mass energies and are then combined at each energy point. The results of this fit, including the SLD results, are given in Appendix A. The dependence of the average asymmetries on centre-of-mass energy agrees with the prediction of the Standard Model. A second fit is made to derive the pole asymmetries $A_{FB}^{0,q}$ from the measured quark asymmetries, in which all the off-peak asymmetry measurements are corrected to the peak energy before combining. This fit determines a total of 14 parameters: the two partial widths, two LEP asymmetries, two coupling parameters

[2] Actually the product $P(c \to D^{*+}) \times BR(D^{*+} \to \pi^+ D^0)$ is fitted because this quantity is needed and measured by the LEP experiments.

from SLD, three semileptonic branching ratios, the average mixing parameter and the probabilities for c quark to fragment into a D^+, a D_s, a D^{*+}, or a charmed baryon. If the SLD measurements are excluded from the fit there are 12 parameters to be determined.

5.1 Summary of Measurements and Averaging Procedure

All measurements are presented by the LEP and SLD collaborations in a consistent manner for the purpose of combination. The tables prepared by the experiments include a detailed breakdown of the systematic error of each measurement and its dependence on other electroweak parameters. Where necessary, the experiments apply small corrections to their results in order to use agreed values and ranges for the input parameters to calculate systematic errors. The measurements, corrected where necessary, are summarised in Appendix A in Tables 20–39, where the statistical and systematic errors are quoted separately. The correlated systematic entries are from physics sources shared with one or more other results in the table and are derived from the full breakdown of common systematic uncertainties. The uncorrelated systematic entries come from the remaining sources.

5.1.1 Averaging Procedure

A χ^2 minimisation procedure is used to derive the values of the heavy-flavour electroweak parameters as published in Reference 3. The full statistical and systematic covariance matrix for all measurements is calculated. This correlation matrix takes into account correlations between different measurements of one experiment and between different experiments. The explicit dependence of each measurement on the other parameters is also accounted for.

Since c-quark events form the main background in the R_b analyses, in the lifetime R_b analyses, the value of R_b depends on the value of R_c. If R_b and R_c are measured in the same analysis, this is reflected in the correlation matrix for the results. However the analyses do not determine R_b and R_c simultaneously but instead measure R_b for an assumed value of R_c. In this case the dependence is parameterised as

$$R_b = R_b^{meas} + a(R_c)\frac{(R_c - R_c^{used})}{R_c}. \quad (12)$$

In this expression, R_b^{meas} is the result of the analysis assuming a value of $R_c = R_c^{used}$. The values of R_c^{used} and the coefficients $a(R_c)$ are given in Table 20 where appropriate. The dependence of all other measurements on other electroweak parameters is treated in the same way, with coefficients $a(x)$ describing the dependence on parameter x.

5.1.2 Partial Width Measurements

The measurements of R_b and R_c fall into two categories. In the first, called a single-tag measurement, a method to select b or c events is devised, and the number of tagged events is counted. This number must then be corrected for backgrounds from other flavours and for the tagging efficiency to calculate the true fraction of hadronic Z decays of that flavour. The dominant systematic errors come from understanding the branching ratios and detection efficiencies which give the overall tagging efficiency. For the second technique, called a double-tag measurement, each event is divided into two hemispheres.

With N_t being the number of tagged hemispheres, N_{tt} the number of events with both hemispheres tagged and N_{had} the total number of hadronic Z decays one has

$$\frac{N_t}{2N_{had}} = \varepsilon_b R_b + \varepsilon_c R_c + \varepsilon_{uds}(1 - R_b - R_c), \quad (13)$$

$$\frac{N_{tt}}{N_{had}} = \mathcal{C}_b \varepsilon_b^2 R_b + \mathcal{C}_c \varepsilon_c^2 R_c + \mathcal{C}_{uds}\varepsilon_{uds}^2(1 - R_b - R_c), \quad (14)$$

where ε_b, ε_c and ε_{uds} are the tagging efficiencies per hemisphere for b, c and light-quark events, and $\mathcal{C}_q \neq 1$ accounts for the fact that the tagging efficiencies between the hemispheres may be correlated. In the case of R_b one has $\varepsilon_b \gg \varepsilon_c \gg \varepsilon_{uds}$, $\mathcal{C}_b \approx 1$. The correlations for the other flavours can be neglected. These equations can be solved to give R_b and ε_b. Neglecting the c and uds backgrounds and the correlations they are approximately given by

$$\varepsilon_b \approx 2N_{tt}/N_t, \quad (15)$$

$$R_b \approx N_t^2/(4N_{tt}N_{had}). \quad (16)$$

The double-tagging method has the advantage that the b tagging efficiency is derived from the data, reducing the systematic error. The residual background of other flavours in the sample, and the evaluation of the correlation between the tagging efficiencies in the two hemispheres of the event are the main sources of systematic uncertainty in such an analysis.

This method can be enhanced by including more tags. All additional efficiencies can be determined from the data, reducing the statistical uncertainties without adding new systematic uncertainties.

Small corrections must be applied to the results to obtain the partial width ratios R_b^0 and R_c^0 from the cross section ratios R_b and R_c. These corrections depend slightly on the invariant mass cutoff of the simulations used by the experiments, so that they are applied by the collaborations before the combination.

The partial width measurements included are:

- Lifetime (and lepton) double tag measurements for R_b from ALEPH [25], DELPHI [26], L3 [27], OPAL [28] and SLD [29]. These are the most precise determinations of R_b. Since they completely dominate the combined result, no other R_b measurements are used at present. The basic features of the double-tag technique are discussed above. In the ALEPH, DELPHI, OPAL and SLD measurements the charm rejection is enhanced by using the invariant mass information. DELPHI, OPAL and SLD also add kinematic information from the particles at the secondary vertex. The ALEPH and DELPHI measurements make use of several different tags; this improves the statistical accuracy and reduces the systematic errors due to hemisphere correlations and charm contamination, compared with the simple single/double tag.
- Analyses with $D/D^{*\pm}$ mesons to measure R_c from ALEPH, DELPHI and OPAL. All measurements are constructed in such a way that no assumptions on the energy dependence of charm fragmentation are necessary. The available measurements can be divided into four groups:
  - inclusive/exclusive double tag (ALEPH [30], DELPHI [31, 32], OPAL [33]): In a first step $D^{*\pm}$ mesons are reconstructed in several decay channels and their production rate is measured, which depends on the product $R_c \times P(c \to D^{*+}) \times BR(D^{*+} \to \pi^+ D^0)$. This sample of $c\bar{c}$ (and $b\bar{b}$) events is then used to measure $P(c \to D^{*+}) \times BR(D^{*+} \to \pi^+ D^0)$ using a slow pion tag in the opposite hemisphere. In the ALEPH measurement R_c is unfolded internally in the analysis so that no explicit $P(c \to D^{*+}) \times BR(D^{*+} \to \pi^+ D^0)$ is available.

– exclusive double tag (ALEPH [30]): This analysis uses exclusively reconstructed D^{*+}, D^0 and D^+ mesons in different decay channels. It has lower statistics but better purity than the inclusive analyses.

– reconstruction of all weakly decaying charmed states (ALEPH [34], DELPHI [32], OPAL [35]): These analyses make the assumption that the production rates of D^0, D^+, D_s and Λ_c in $c\bar{c}$ events add up to one with small corrections due to unmeasured charms strange baryons. This is a single tag measurement, relying only on knowing the decay branching ratios of the charm hadrons. These analyses are also used to measure the c hadron production ratios which are needed for the R_b analyses.

- A lifetime plus mass double tag from SLD to measure R_c [29]. This analysis uses the same tagging algorithm as the SLD R_b analysis, but with the neural net tuned to tag charm. Although the charm tag has a purity of about 84%, most of the background is from b which can be measured with high precision from the b/c mixed tag rate.

- A measurement of R_c using single leptons assuming $BR(c \to \ell)$ from ALEPH [30].

To avoid effects from non linearities in the fit, for the inclusive/exclusive single/double tag and for the charm-counting analyses, the products $R_c P(c \to D^{*+}) \times BR(D^{*+} \to \pi^+ D^0)$, $R_c f_{D^0}$, $R_c f_{D^+}$, $R_c f_{D_s}$ and $R_c f_{\Lambda_c}$that are actually measured in the analyses are directly used as inputs to the fit. The measurements of the production rates of weakly decaying charmed hadrons, especially $R_c f_{D_s}$ and $R_c f_{\Lambda_c}$ have a substantial error due to the branching ratio of the decay mode used. Since this error is a relative one there is a potential bias towards lower measurements. To avoid this bias, for the production rates of weakly decaying charmed hadrons the logarithm of the production rates instead of the rates themselves are input to the fit. For $R_c f_{D^0}$ and $R_c f_{D^+}$ the difference between the results using the logarithm or the value itself is negligible. For $R_c f_{D_s}$ and $R_c f_{\Lambda_c}$ the difference in the R_c-result is about one tenth of a standard deviation.

5.1.3 Asymmetry Measurements

All b and c asymmetries given by the experiments are corrected to full acceptance.

The QCD corrections to the forward-backward asymmetries depend strongly on the experimental analyses. For this reason the numbers given by the collaborations are also corrected for QCD effects. A detailed description of the procedure can be found in [36] with updates reported in [24]

For the 12- and 14-parameter fits described above, the LEP peak and off-peak asymmetries are corrected to $\sqrt{s} = 91.26$ GeV using the predicted dependence from ZFITTER [37]. The slope of the asymmetry around m_Z depends only on the axial coupling and the charge of the initial and final state fermions and is thus independent of the value of the asymmetry itself.

After calculating the overall averages, the quark pole asymmetries, $A_{FB}^{0,q}$, are derived by applying the corrections described below. To relate the pole asymmetries to the measured ones a few corrections that are summarised in Table 8 have to be applied. These corrections are due to the energy shift from 91.26 GeV to m_Z, initial state radiation, γ exchange and γ-Z interference. A very small correction due to the nonzero value of the b quark mass is included in the correction called γ-Z interference. All corrections are calculated using ZFITTER.

The SLD left-right-forward-backward asymmetries are also corrected for all radiative effects and are directly presented in terms of $\mathcal{A}_b$ and $\mathcal{A}_c$.

Source	δA_{FB}^b	δA_{FB}^c
$\sqrt{s} = m_Z$	-0.0013	-0.0034
QED corrections	$+0.0041$	$+0.0104$
γ, γ-Z, mass	-0.0003	-0.0008
Total	$+0.0025$	$+0.0062$

Table 8: Corrections to be applied to the quark asymmetries as $A_{FB}^0 = A_{FB}^{meas} + \delta A_{FB}$.

The measurements used are:

- Measurements of $A_{FB}^{b\bar{b}}$ and $A_{FB}^{c\bar{c}}$ using leptons from ALEPH [38], DELPHI [39], L3 [40] and OPAL [41]. These analyses measure either $A_{FB}^{b\bar{b}}$ only from a high p_t lepton sample or they obtain $A_{FB}^{b\bar{b}}$ and $A_{FB}^{c\bar{c}}$ from a fit to the lepton spectra. In the case of OPAL the lepton information is combined with hadronic variables in a neural net. DELPHI uses in addition lifetime information and jet-charge in the hemisphere opposite to the lepton to separate the different lepton sources. Some asymmetry analyses also measure $\overline{\chi}$.

- Measurements of $A_{FB}^{b\bar{b}}$ based on lifetime tagged events with a hemisphere charge measurement from ALEPH [42], DELPHI [43, 44], L3 [45] and OPAL [46]. These measurements contribute roughly the same weight to the combined result as the lepton fits.

- Analyses with D mesons to measure $A_{FB}^{c\bar{c}}$ from ALEPH [47] or $A_{FB}^{c\bar{c}}$ and $A_{FB}^{b\bar{b}}$ from DELPHI [48] and OPAL [49].

- Measurements of $\mathcal{A}_b$ and $\mathcal{A}_c$ from SLD. These results include measurements using lepton [50,51], D meson [52] and vertex mass plus hemisphere charge [53] tags, which have similar sources of systematic errors as the LEP asymmetry measurements. SLD also uses vertex mass for bottom or charm tag in conjunction with a kaon tag or a vertex charge tag for both $\mathcal{A}_b$ and $\mathcal{A}_c$ measurements [54–56].

5.1.4 Other Measurements

The measurements of the charmed hadron fractions $P(c \to D^{*+}) \times BR(D^{*+} \to \pi^+ D^0)$, $f(D^+)$, $f(D_s)$ and $f(c_{baryon})$ are included in the R_c measurements and are described there.

ALEPH [57], DELPHI [58], L3 [27, 59] and OPAL [60] measure $BR(b \to \ell)$, $BR(b \to c \to \bar{\ell})$ and $\overline{\chi}$ or a subset of them from a sample of leptons opposite to a b-tagged hemisphere and from a double lepton sample. DELPHI [31] and OPAL [61] measure $BR(c \to \ell)$ from a sample opposite to a high energy $D^{*\pm}$.

5.2 Results

5.2.1 Results of the 12-Parameter Fit to the LEP Data

Using the full averaging procedure gives the following combined results for the electroweak parameters:

$$R_b^0 = 0.21654 \pm 0.00074 \quad (17)$$

$$
\begin{aligned}
R_{\rm c}^0 &= 0.1689 \pm 0.0047 \\
A_{\rm FB}^{0,\,{\rm b}} &= 0.0982 \pm 0.0017 \\
A_{\rm FB}^{0,\,{\rm c}} &= 0.0688 \pm 0.0035\,,
\end{aligned}
$$

where all corrections to the asymmetries and partial widths are applied. The χ^2/d.o.f. is $46/(90-12)$. The corresponding correlation matrix is given in Table 9.

	$R_{\rm b}^0$	$R_{\rm c}^0$	$A_{\rm FB}^{0,\,{\rm b}}$	$A_{\rm FB}^{0,\,{\rm c}}$
$R_{\rm b}^0$	1.00	−0.16	−0.10	0.02
$R_{\rm c}^0$	−0.16	1.00	0.06	−0.01
$A_{\rm FB}^{0,\,{\rm b}}$	−0.10	0.06	1.00	0.16
$A_{\rm FB}^{0,\,{\rm c}}$	0.02	−0.01	0.16	1.00

Table 9: The correlation matrix for the four electroweak parameters from the 12-parameter fit.

5.2.2 Results of the 14-Parameter Fit to LEP and SLD Data

Including the SLD results for $R_{\rm b}$, $R_{\rm c}$, $\mathcal{A}_{\rm b}$ and $\mathcal{A}_{\rm c}$ into the fit the following results are obtained:

$$
\begin{aligned}
R_{\rm b}^0 &= 0.21664 \pm 0.00068 \\
R_{\rm c}^0 &= 0.1729 \pm 0.0032 \\
A_{\rm FB}^{0,\,{\rm b}} &= 0.0982 \pm 0.0017 \\
A_{\rm FB}^{0,\,{\rm c}} &= 0.0689 \pm 0.0035 \\
\mathcal{A}_{\rm b} &= 0.921 \pm 0.020 \\
\mathcal{A}_{\rm c} &= 0.667 \pm 0.026\,,
\end{aligned}
\qquad (18)
$$

with a χ^2/d.o.f. of $50/(99-14)$. The corresponding correlation matrix is given in Table 10 and the largest errors for the electroweak parameters are listed in Table 11.

In deriving these results the parameters $\mathcal{A}_{\rm b}$ and $\mathcal{A}_{\rm c}$ are treated as independent of the forward-backward asymmetries $A_{\rm FB}^{0,\,{\rm b}}$ and $A_{\rm FB}^{0,\,{\rm c}}$. In Figure 2 the results for $R_{\rm b}^0$ and $R_{\rm c}^0$ are shown compared with the Standard Model expectation.

	$R_{\rm b}^0$	$R_{\rm c}^0$	$A_{\rm FB}^{0,\,{\rm b}}$	$A_{\rm FB}^{0,\,{\rm c}}$	$\mathcal{A}_{\rm b}$	$\mathcal{A}_{\rm c}$
$R_{\rm b}^0$	1.00	−0.16	−0.09	0.01	−0.06	0.02
$R_{\rm c}^0$	−0.16	1.00	0.04	−0.02	0.03	−0.04
$A_{\rm FB}^{0,\,{\rm b}}$	−0.09	0.04	1.00	0.16	0.02	0.00
$A_{\rm FB}^{0,\,{\rm c}}$	0.01	−0.02	0.16	1.00	0.00	0.01
$\mathcal{A}_{\rm b}$	−0.06	0.03	0.02	0.00	1.00	0.12
$\mathcal{A}_{\rm c}$	0.02	−0.04	0.00	0.01	0.12	1.00

Table 10: The correlation matrix for the six electroweak parameters from the 14-parameter fit.

The 14 parameter fit yields the $\rm b \to \ell$ branching ratio:

$$
{\rm BR(b \to \ell)} \;=\; 0.1057 \pm 0.0019. \qquad (19)
$$

	$R_{\rm b}^0$ (10^{-3})	$R_{\rm c}^0$ (10^{-3})	$A_{\rm FB}^{0,\,{\rm b}}$ (10^{-3})	$A_{\rm FB}^{0,\,{\rm c}}$ (10^{-3})	$\mathcal{A}_{\rm b}$ (10^{-2})	$\mathcal{A}_{\rm c}$ (10^{-2})
statistics	0.44	2.4	1.5	3.0	1.5	2.1
internal systematics	0.29	1.4	0.7	1.4	1.3	1.6
QCD effects	0.18	0	0.2	0.1	0.4	0.2
BR(D → neut.)	0.14	0.1	0	0	0	0
D decay multiplicity	0.13	0.2	0	0	0	0
$\rm BR(D^+ \to K^-\pi^+\pi^+)$	0.09	0.2	0.1	0	0	0
$\rm BR(D_s \to \phi\pi^+)$	0.03	0.6	0.1	0	0	0
$\rm BR(\Lambda_c \to p\ K^-\pi^+)$	0.06	0.4	0.1	0.1	0	0
D lifetimes	0.06	0.1	0	0.1	0	0
gluon splitting	0.26	.10	0	0.2	0.1	0.1
c fragmentation	0.10	0.2	0.1	0.2	0.1	0.1
light quarks	0.07	0.2	0.1	0.1	0	0
total	0.68	3.2	1.7	3.5	2.0	2.6

Table 11: The dominant error sources for the electroweak parameters from the 14-parameter fit.

The largest error sources on this quantity are the dependences on the semileptonic decay models $\rm b \to \ell$, $\rm c \to \ell$ with

$$
\begin{aligned}
\Delta{\rm BR(b \to \ell)}|_{({\rm b}\to\ell){\rm model}} &= 0.0008, \\
\Delta{\rm BR(b \to \ell)}|_{({\rm c}\to\ell){\rm model}} &= 0.0005.
\end{aligned}
$$

Extensive studies are made to understand the size of these errors. If all the asymmetry measurements are excluded from the fit a consistent result is obtained with modelling errors of 0.0010 and 0.0006. The reduction of the modelling uncertainty is due to the inclusion of asymmetry measurements using different methods. Those using leptons depend on the semileptonic decay models while those using a lifetime tag and jet charge or D mesons do not. The mutual consistency of the asymmetry measurements effectively constrains the semileptonic decay models, and reduces the uncertainty in the semileptonic branching ratio.

The result of the full fit to the LEP+SLC results including the off-peak asymmetries and the non-electroweak parameters can be found in Appendix A. Results for the non-electroweak parameters are independent of the treatment of the off-peak asymmetries and the SLD data.

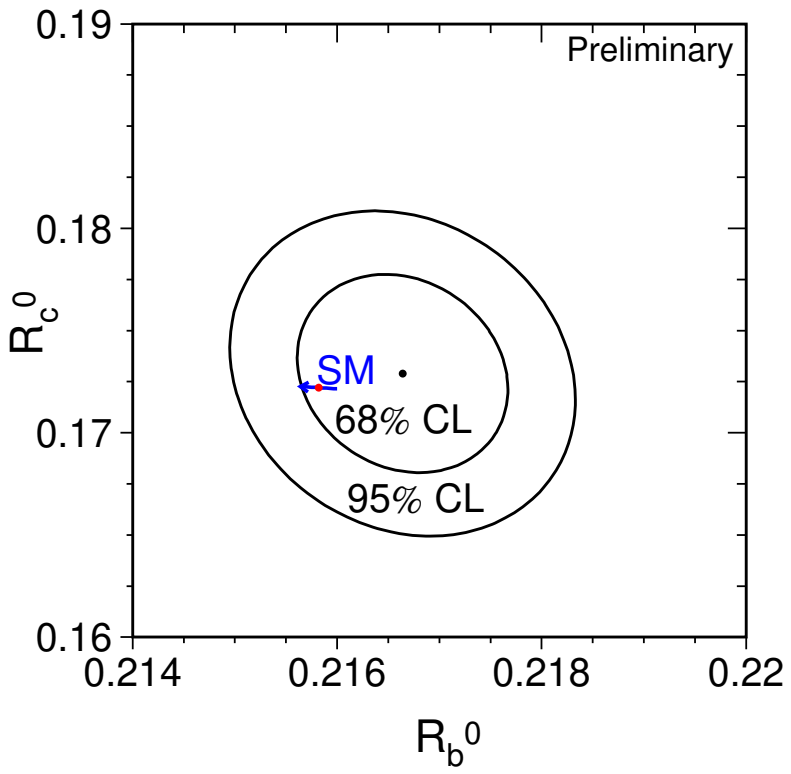

Figure 2: Contours in the R_b^0-R_c^0 plane derived from the LEP+SLD data, corresponding to 68% and 95% confidence levels assuming Gaussian systematic errors. The Standard Model prediction for $m_t = 174.3 \pm 5.1$ GeV is also shown. The arrow points in the direction of increasing values of m_t.

6 The Hadronic Charge Asymmetry $\langle Q_{FB} \rangle$

Updates with respect to last summer:
OPAL reverts to their published result.

The LEP experiments ALEPH [62–64], DELPHI [65,66], L3 [45] and OPAL [67] have provided measurements of the hadronic charge asymmetry based on the mean difference in jet charges measured in the forward and backward event hemispheres, $\langle Q_{FB} \rangle$. DELPHI have also provided a related measurement of the total charge asymmetry by making a charge assignment on an event-by-event basis and performing a likelihood fit [65]. The experimental values quoted for the average forward-backward charge difference, $\langle Q_{FB} \rangle$, cannot be directly compared as some of them include detector dependent effects such as acceptances and efficiencies. Therefore the effective electroweak mixing angle, $\sin^2\theta_{eff}^{lept}$, as defined in Section 12.4, is used as a means of combining the experimental results summarised in Table 12.

Experiment		$\sin^2\theta_{eff}^{lept}$
ALEPH	(90-94), final	$0.2322 \pm 0.0008 \pm 0.0011$
DELPHI	(91-94), prel.	$0.2311 \pm 0.0010 \pm 0.0014$
L3	(91-95), final	$0.2327 \pm 0.0012 \pm 0.0013$
OPAL	(90-91), final	$0.2326 \pm 0.0012 \pm 0.0029$
LEP Average		0.2322 ± 0.0010

Table 12: Summary of the determination of $\sin^2\theta_{eff}^{lept}$ from inclusive hadronic charge asymmetries at LEP. For each experiment, the first error is statistical and the second systematic. The latter is dominated by fragmentation and decay modelling uncertainties.

The dominant source of systematic error arises from the modelling of the charge flow in the fragmentation process for each flavour. All experiments measure the required charge properties for $Z \to b\bar{b}$ events from the data. ALEPH also determines the charm charge properties from the data. The fragmentation model implemented in the JETSET Monte Carlo program [68] is used by all experiments as reference; the one of the HERWIG Monte Carlo program [69] is used for comparison. The JETSET fragmentation parameters are varied to estimate the systematic errors. The central values chosen by the experiments for these parameters are, however, not the same. The smaller of the two fragmentation errors in any pair of results is treated as common to both. The present average of $\sin^2\theta_{eff}^{lept}$ from $\langle Q_{FB} \rangle$ and its associated error are not very sensitive to the treatment of common uncertainties. The ambiguities due to QCD corrections may cause changes in the derived value of $\sin^2\theta_{eff}^{lept}$. These are, however, well below the fragmentation uncertainties and experimental errors. The effect of fully correlating the estimated systematic uncertainties from this source between the experiments has a negligible effect upon the average and its error.

There is also some correlation between these results and those for $A_{FB}^{b\bar{b}}$ using jet charges. The dominant source of correlation is again through uncertainties in the fragmentation and decay models used. The typical correlation between the derived values of $\sin^2\theta_{eff}^{lept}$ from the $\langle Q_{FB} \rangle$ and the $A_{FB}^{b\bar{b}}$ jet charge measurements is estimated to be about 20% to 25%. This leads to only a small change in the relative weights for the $A_{FB}^{b\bar{b}}$ and $\langle Q_{FB} \rangle$ results when averaging their $\sin^2\theta_{eff}^{lept}$ values (Section 12.4). Furthermore, the jet charge method contributes at most half of the weight of the $A_{FB}^{b\bar{b}}$ measurement. Thus, the correlation between $\langle Q_{FB} \rangle$ and $A_{FB}^{b\bar{b}}$ from jet charge will have little impact on the overall Standard Model fit, and is neglected at present.

7 Fermion-Pair Production at LEP-II

Updates with respect to last summer:
Additional preliminary results based on the data collected in the year 2000 are included.

Please see `http://lepewwg.web.cern.ch/LEPEWWG/lep2/moriond2001/Welcome.html` for the most recent summary.

8 Measurement of W Boson Properties at LEP-II

Updates with respect to last summer:
Additional preliminary results based on the data collected in the year 2000 are included.

Please see `http://lepewwg.web.cern.ch/LEPEWWG/lepww/4f/Winter01/` for the most recent summary on W-pair production cross sections and W decay branching fractions.

Please see `http://lepewwg.web.cern.ch/LEPEWWG/lepww/mw/Winter01/` for the most recent summary on W mass and total width.

9 Single-W Production Cross Section

Updates with respect to last summer:
ALEPH have presented preliminary measurements based on the year 2000 data.

Please see `http://lepewwg.web.cern.ch/LEPEWWG/lepww/4f/Winter01/` for the most recent summary.

10 ZZ Production Cross Section

Updates with respect to last summer:
Additional preliminary results based on the data collected in the year 2000 are included.

Please see `http://lepewwg.web.cern.ch/LEPEWWG/lepww/4f/Winter01/` for the most recent summary.

11 Electroweak Gauge Boson Couplings

Updates with respect to last summer:
Additional preliminary results based on the data collected in the year 2000 are included.

Please see `http://lepewwg.web.cern.ch/LEPEWWG/lepww/tgc/` for the most recent summary.

12 Interpretation of Results

Updates with respect to last summer:
Effective vector and axial-vector couplings constants are also determined for the heavy quark flavours

12.1 Number of Neutrino Species

An important aspect of our measurement concerns the information related to Z decays into invisible channels. Using the results of Table 3, the ratio of the Z decay width into invisible particles and the leptonic decay width is determined:

$$\Gamma_{\rm inv}/\Gamma_{\ell\ell} \;=\; 5.942 \pm 0.016\,. \tag{20}$$

The Standard Model value for the ratio of the partial widths to neutrinos and charged leptons is:

$$(\Gamma_{\nu\nu}/\Gamma_{\ell\ell})_{\rm SM} \;=\; 1.9912 \pm 0.0012\,. \tag{21}$$

The central value is evaluated for $m_{\rm Z} = 91.1875$ GeV and the error quoted accounts for a variation of $m_{\rm t}$ in the range $m_{\rm t} = 174.3 \pm 5.1$ GeV and a variation of $m_{\rm H}$ in the range 100 GeV $\leq m_{\rm H} \leq$ 1000 GeV. The number of light neutrino species is given by the ratio of the two expressions listed above:

$$N_\nu \;=\; 2.9841 \pm 0.0083, \tag{22}$$

which is 2 standard deviations below the expected value of 3.

Alternatively, one can assume 3 neutrino species and determine the width from additional invisible decays of the Z. This yields

$$\Delta\Gamma_{\rm inv} \;=\; -2.7 \pm 1.6 \text{ MeV}. \tag{23}$$

The measured total width is below the Standard Model expectation. If a conservative approach is taken to limit the result to only positive values of $\Delta\Gamma_{\rm inv}$, then the 95% CL upper limit on additional invisible decays of the Z is

$$\Delta\Gamma_{\rm inv} \;<\; 2.0 \text{ MeV}. \tag{24}$$

The uncertainties on N_ν and $\Delta\Gamma_{\rm inv}$ are dominated by the theoretical error on the luminosity. These results have therefore improved due to the improved theoretical calculations on Bhabha scattering [14].

12.2 The Coupling Parameters $\mathcal{A}_{\rm f}$

The coupling parameters $\mathcal{A}_{\rm f}$ are defined in terms of the effective vector and axial-vector neutral current couplings of fermions (Equation (4)). The LEP measurements of the forward-backward asymmetries of charged leptons (Section 2) and b and c quarks (Section 5) determine the products $A_{\rm FB}^{0,\rm f} = \frac{3}{4}\mathcal{A}_{\rm e}\mathcal{A}_{\rm f}$ (Equation (3)). The LEP measurements of the τ polarisation (Section 3), $\mathcal{P}_\tau(\cos\theta)$, determine $\mathcal{A}_\tau$ and $\mathcal{A}_{\rm e}$ separately (Equation (6)).

Table 13 shows the results for the leptonic coupling parameter $\mathcal{A}_\ell$ from the LEP and SLD measurements, assuming lepton universality.

	$\mathcal{A}_\ell$	Cumulative Average	χ^2/d.o.f.
$A_{\rm FB}^{0,\ell}$	0.1512 ± 0.0042		
$\mathcal{P}_\tau(\cos\theta)$	0.1464 ± 0.0031	0.1480 ± 0.0025	0.8/1
$\mathcal{A}_\ell$ (SLD)	0.1513 ± 0.0021	0.1500 ± 0.0016	1.7/2

Table 13: Determination of the leptonic coupling parameter $\mathcal{A}_\ell$ assuming lepton universality. The second column lists the $\mathcal{A}_\ell$ values derived from the quantities listed in the first column. The third column contains the cumulative averages of these $\mathcal{A}_\ell$ results. The averages are derived assuming no correlations between the measurements. The χ^2 per degree of freedom for the cumulative averages is given in the last column.

	LEP ($\mathcal{A}_\ell = 0.1480 \pm 0.0025$)	SLD	LEP+SLD ($\mathcal{A}_\ell = 0.1500 \pm 0.0016$)	Standard Model fit
$\mathcal{A}_{\rm b}$	0.884 ± 0.022	0.921 ± 0.020	0.896 ± 0.013	0.935
$\mathcal{A}_{\rm c}$	0.620 ± 0.033	0.667 ± 0.026	0.647 ± 0.020	0.668

Table 14: Determination of the quark coupling parameters $\mathcal{A}_{\rm b}$ and $\mathcal{A}_{\rm c}$ from LEP data alone (using the LEP average for $\mathcal{A}_\ell$), from SLD data alone, and from LEP+SLD data (using the LEP+SLD average for $\mathcal{A}_\ell$) assuming lepton universality.

Using the measurements of $\mathcal{A}_\ell$ one can extract $\mathcal{A}_{\rm b}$ and $\mathcal{A}_{\rm c}$ from the LEP measurements of the b and c quark asymmetries. The SLD measurements of the left-right forward-backward asymmetries for b and c quarks are direct determinations of $\mathcal{A}_{\rm b}$ and $\mathcal{A}_{\rm c}$. Table 14 shows the results on the quark coupling parameters $\mathcal{A}_{\rm b}$ and $\mathcal{A}_{\rm c}$ derived from LEP or SLD measurements separately (Equations 17 and 18) and from the combination of LEP+SLD measurements (Equation 18).

The LEP extracted values of $\mathcal{A}_{\rm b}$ and $\mathcal{A}_{\rm c}$ are in agreement with the SLD measurements, but somewhat lower than the Standard Model predictions (0.935 and 0.668, respectively, essentially independent of $m_{\rm t}$ and $m_{\rm H}$). The combination of LEP and SLD of $\mathcal{A}_{\rm b}$ is 3.0 sigma below the Standard Model, while $\mathcal{A}_{\rm c}$ agrees at the 1.0 sigma level. This is mainly because the $\mathcal{A}_{\rm b}$ value, deduced from the measured $A_{\rm FB}^{0,\rm b}$ and the combined $\mathcal{A}_\ell$, is significantly lower than both the Standard Model and the direct measurement of $\mathcal{A}_{\rm b}$, this can also be seen in Figure 3.

12.3 The Effective Vector and Axial-Vector Coupling Constants

The partial widths of the Z into leptons and the lepton forward-backward asymmetries (Section 2), the τ polarisation and the τ polarisation asymmetry (Section 3) are combined to determine the effective vector and axial-vector couplings for e, μ and τ. The asymmetries (Equations (3) and (6)) determine the ratio $g_{V\ell}/g_{A\ell}$ (Equation (4)), while the leptonic partial widths determine the sum of the squares of the couplings:

$$\Gamma_{\ell\ell} \;=\; \frac{G_{\rm F} m_{\rm Z}^3}{6\pi\sqrt{2}}(g_{V\ell}^2 + g_{A\ell}^2)(1+\delta_\ell^{QED})\,, \qquad (25)$$

where $\delta_\ell^{QED} = 3q_\ell^2\alpha(m_{\rm Z}^2)/(4\pi)$ accounts for final state photonic corrections. Corrections due to lepton masses, neglected in Equation 25, are taken into account for the results presented below.

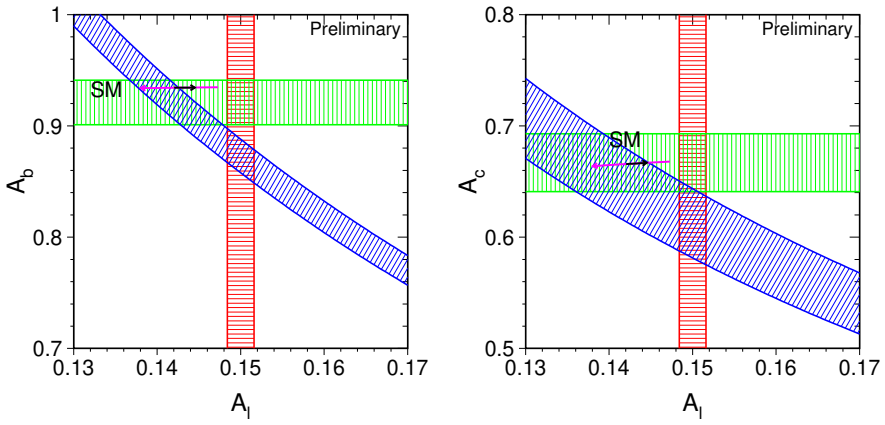

Figure 3: The measurements of the combined LEP+SLD $\mathcal{A}_\ell$ (vertical band), SLD $\mathcal{A}_{\rm b}$,$\mathcal{A}_{\rm c}$ (horizontal bands) and LEP $A_{\rm FB}^{0,\rm b}$,$A_{\rm FB}^{0,\rm c}$ (diagonal bands), compared to the Standard Model expectations (arrows). The arrow pointing to the left shows the variation in the SM prediction for $m_{\rm H}$ in the range 300^{+700}_{-187} GeV, and the arrow pointing to the right for $m_{\rm t}$ in the range 174.3 ± 5.1 GeV. Although the $A_{\rm FB}^{0,\rm b}$ measurements prefer a high Higgs mass, the Standard Model fit to the full set of measurements prefers a low Higgs mass, for example because of the influence of $\mathcal{A}_\ell$.

The averaged results for the effective lepton couplings are given in Table 15 for both the LEP data alone as well as for the LEP and SLD measurements. Figure 4 shows the 68% probability contours in the $g_{A\ell}$-$g_{V\ell}$ plane for the individual lepton species from the LEP data. The signs of $g_{A\ell}$ and $g_{V\ell}$ are based on the convention $g_{Ae} < 0$. With this convention the signs of the couplings of all charged leptons follow from LEP data alone. For comparison, the $g_{V\ell}$-$g_{A\ell}$ relation following from the measurement of $\mathcal{A}_\ell$ from SLD [70] is indicated as a band in the $g_{A\ell}$-$g_{V\ell}$-plane of Figure 4. The measured ratios of the e, μ and τ couplings provide a test of lepton universality and are shown in Table 15. All values are consistent with lepton universality. The combined results assuming universality are also given in the table and are shown as a solid contour in Figure 4.

The neutrino couplings to the Z can be derived from the measured value of the invisible width of the Z, $\Gamma_{\rm inv}$ (see Table 4), attributing it exclusively to the decay into three identical neutrino generations ($\Gamma_{\rm inv} = 3\Gamma_{\nu\nu}$) and assuming $g_{A\nu} \equiv g_{V\nu} \equiv g_\nu$. The relative sign of g_ν is chosen to be in agreement with neutrino scattering data [71], resulting in $g_\nu = +0.50068 \pm 0.00075$.

The couplings analysis is extended to include also the heavy flavour measurements as presented in Section 5.2. Assuming neutral-current lepton universality, the effective coupling constants are determined jointly for leptons as well as for b and c quarks. The results are also reported in Table 15 and shown in Figure 5. The deviation of the b-quark couplings from the Standard-Model expectation is mainly caused by the combined value of $\mathcal{A}_{\rm b}$ being low as discussed in Section 12.2 and shown in Figure 3.

	Without Lepton Universality:	
	LEP	LEP+SLD
$g_{V\mathrm{e}}$	-0.0378 ± 0.0011	-0.03816 ± 0.00047
$g_{V\mu}$	-0.0376 ± 0.0031	-0.0367 ± 0.0023
$g_{V\tau}$	-0.0367 ± 0.0010	-0.03654 ± 0.00097
$g_{A\mathrm{e}}$	-0.50112 ± 0.00035	-0.50111 ± 0.00035
$g_{A\mu}$	-0.50115 ± 0.00056	-0.50120 ± 0.00054
$g_{A\tau}$	-0.50205 ± 0.00064	-0.50204 ± 0.00064
	Ratios of couplings:	
	LEP	LEP+SLD
$g_{V\mu}/g_{V\mathrm{e}}$	0.995 ± 0.096	0.962 ± 0.063
$g_{V\tau}/g_{V\mathrm{e}}$	0.971 ± 0.040	0.957 ± 0.028
$g_{A\mu}/g_{A\mathrm{e}}$	1.0001 ± 0.0014	1.0002 ± 0.0014
$g_{A\tau}/g_{A\mathrm{e}}$	1.0018 ± 0.0015	1.0019 ± 0.0015
	With Lepton Universality:	
	LEP	LEP+SLD
$g_{V\ell}$	-0.03732 ± 0.00064	-0.03781 ± 0.00041
$g_{A\ell}$	-0.50127 ± 0.00026	-0.50123 ± 0.00026
g_{ν}	$+0.50068 \pm 0.00075$	$+0.50068 \pm 0.00075$
	With Lepton Universality and Heavy Flavour Results:	
	LEP	LEP+SLD
$g_{V\ell}$	-0.03731 ± 0.00064	-0.03750 ± 0.00038
$g_{V\mathrm{b}}$	-0.314 ± 0.012	-0.3200 ± 0.0078
$g_{V\mathrm{c}}$	$+0.175 \pm 0.011$	$+0.1854 \pm 0.0069$
$g_{A\ell}$	-0.50126 ± 0.00026	-0.50125 ± 0.00026
$g_{A\mathrm{b}}$	-0.5200 ± 0.0074	-0.5162 ± 0.0051
$g_{A\mathrm{c}}$	$+0.5027 \pm 0.0079$	$+0.5055 \pm 0.0054$

Table 15: Results for the effective vector and axial-vector couplings derived from the LEP data and the combined LEP and SLD data without and with the assumption of lepton universality. Note that the results for b-quarks are highly correlated.

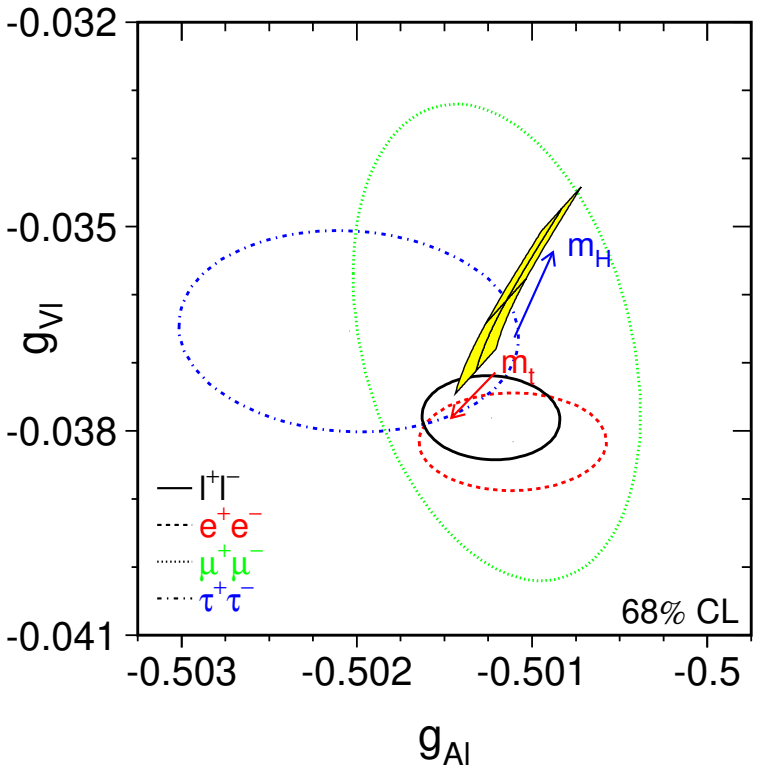

Figure 4: Contours of 68% probability in the $g_{V\ell}$-$g_{A\ell}$ plane from LEP and SLD measurements. The solid contour results from a fit to the LEP and SLD results assuming lepton universality. The shaded region corresponds to the Standard Model prediction for $m_{\mathrm{t}} = 174.3 \pm 5.1$ GeV and $m_{\mathrm{H}} = 300^{+700}_{-187}$ GeV. The arrows point in the direction of increasing values of m_{t} and m_{H}.

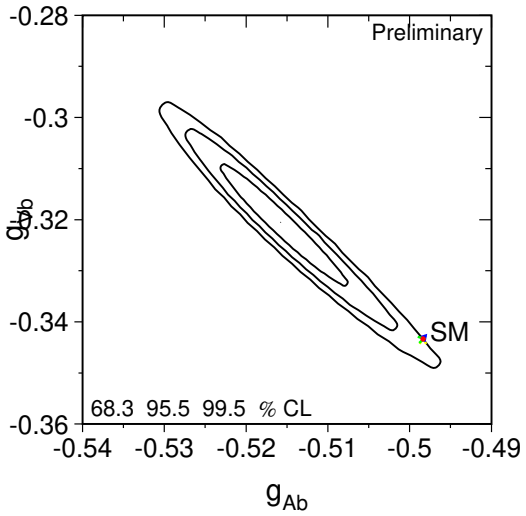

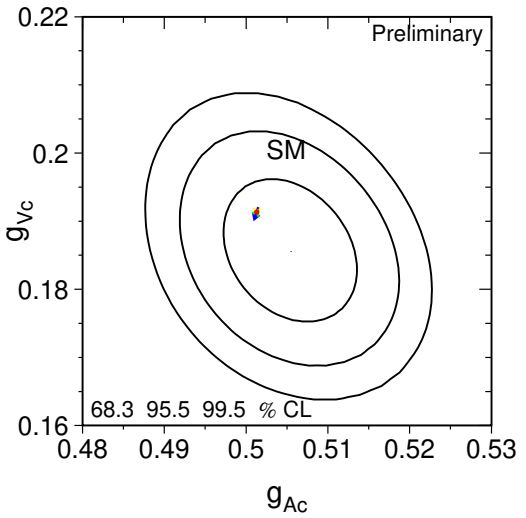

Figure 5: Contours of 68.3, 95.5 and 99.5% probability in the $g_{V\mathrm{q}}$-$g_{A\mathrm{q}}$ plane from LEP and SLD measurements for b and c quarks and assuming lepton universality. The dot corresponds to the Standard Model prediction for $m_{\mathrm{t}} = 174.3 \pm 5.1$ GeV and $m_{\mathrm{H}} = 300^{+700}_{-187}$ GeV.

12.4 The Leptonic Effective Electroweak Mixing Angle $\sin^2\theta^{\mathrm{lept}}_{\mathrm{eff}}$

The asymmetry measurements from LEP and SLD can be combined into a single observable, the effective electroweak mixing angle, $\sin^2\theta^{\mathrm{lept}}_{\mathrm{eff}}$, defined as:

$$\sin^2\theta^{\mathrm{lept}}_{\mathrm{eff}} \equiv \frac{1}{4}\left(1 - \frac{g_{V\ell}}{g_{A\ell}}\right), \tag{26}$$

without making strong model-specific assumptions.

For a combined average of $\sin^2\theta^{\mathrm{lept}}_{\mathrm{eff}}$ from $A^{0,\ell}_{\mathrm{FB}}$, $\mathcal{A}_\tau$ and $\mathcal{A}_{\mathrm{e}}$ only the assumption of lepton universality, already inherent in the definition of $\sin^2\theta^{\mathrm{lept}}_{\mathrm{eff}}$, is needed. Also the value derived from the measurements of $\mathcal{A}_\ell$ from SLD is given. We also include the hadronic forward-backward asymmetries, assuming the quark couplings to be given by the Standard Model. This is justified within the Standard Model as the hadronic asymmetries $A^{0,\mathrm{b}}_{\mathrm{FB}}$ and $A^{0,\mathrm{c}}_{\mathrm{FB}}$ have a reduced sensitivity to corrections particular to the quark vertex. The results of these determinations of $\sin^2\theta^{\mathrm{lept}}_{\mathrm{eff}}$ and their combination are shown in Table 16 and in Figure 6. The combinations based on leptonic and hadronic results show a difference of 3.6 sigma, mainly caused by the two most precise measurements of $\sin^2\theta^{\mathrm{lept}}_{\mathrm{eff}}$, A^0_{LR} (SLD) and $A^{0,\mathrm{b}}_{\mathrm{FB}}$ (LEP). This is the same effect as discussed already in sections 12.2 and 12.3 and shown in Figures 3 and 5: the deviation in $\mathcal{A}_{\mathrm{b}}$ as extracted from $A^{0,\mathrm{b}}_{\mathrm{FB}}$ discussed above is reflected in the value of $\sin^2\theta^{\mathrm{lept}}_{\mathrm{eff}}$ extracted from $A^{0,\mathrm{b}}_{\mathrm{FB}}$ in this analysis.

	$\sin^2\theta^{\mathrm{lept}}_{\mathrm{eff}}$	Average by Group of Observations	Cumulative Average	χ^2/d.o.f.
$A^{0,\ell}_{\mathrm{FB}}$	0.23099 ± 0.00053			
$\mathcal{A}_\tau$	0.23192 ± 0.00052			
$\mathcal{A}_{\mathrm{e}}$	0.23117 ± 0.00061	0.23139 ± 0.00032	0.23139 ± 0.00032	1.7/2
$\mathcal{A}_\ell$ (SLD)	0.23098 ± 0.00026	0.23098 ± 0.00026	0.23114 ± 0.00020	2.7/3
$A^{0,\mathrm{b}}_{\mathrm{FB}}$	0.23240 ± 0.00031			
$A^{0,\mathrm{c}}_{\mathrm{FB}}$	0.23262 ± 0.00080			
$\langle Q_{\mathrm{FB}} \rangle$	0.2322 ± 0.0010	0.23240 ± 0.00029	0.23156 ± 0.00017	15.5/6

Table 16: Determinations of $\sin^2\theta^{\mathrm{lept}}_{\mathrm{eff}}$ from asymmetries. The second column lists the $\sin^2\theta^{\mathrm{lept}}_{\mathrm{eff}}$ values derived from the quantities listed in the first column. The third column contains the averages of these numbers by groups of observations, where the groups are separated by the horizontal lines. The fourth column shows the cumulative averages. The χ^2 per degree of freedom for the cumulative averages is also given. The averages have been performed including the small correlation between $A^{0,\mathrm{b}}_{\mathrm{FB}}$ and $A^{0,\mathrm{c}}_{\mathrm{FB}}$.

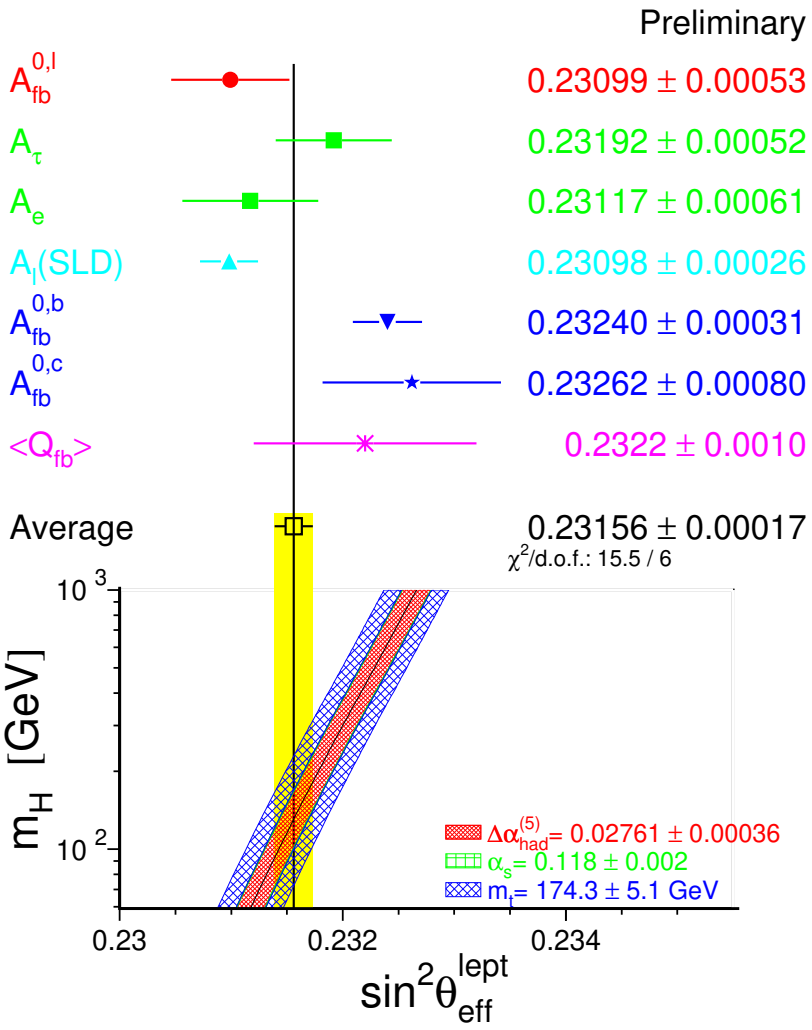

Figure 6: Comparison of several determinations of $\sin^2\theta_{\rm eff}^{\rm lept}$ from asymmetries. In the average, the small correlation between $A_{\rm FB}^{0,\,\rm b}$ and $A_{\rm FB}^{0,\,\rm c}$ is included. Also shown is the prediction of the Standard Model as a function of $m_{\rm H}$. The width of the Standard Model band is due to the uncertainties in $\Delta\alpha_{\rm had}^{(5)}(m_{\rm Z}^2)$ (see Section 12.5), $\alpha_{\rm s}(m_{\rm Z}^2)$ and $m_{\rm t}$. The total width of the band is the linear sum of these effects.

12.5 Constraints on the Standard Model

The precise electroweak measurements performed at LEP and SLC and elsewhere can be used to check the validity of the Standard Model and, within its framework, to infer valuable information about its fundamental parameters. The accuracy of the measurements makes them sensitive to the mass of the top quark $m_{\rm t}$, and to the mass of the Higgs boson $m_{\rm H}$ through loop corrections. While the leading $m_{\rm t}$ dependence is quadratic, the leading $m_{\rm H}$ dependence is logarithmic. Therefore, the inferred constraints on $m_{\rm H}$ are not very strong.

12.5.1 Inputs

The LEP and SLD measurements used are summarised in Table 17 together with the results of the Standard Model fit. Also shown are the results of measurements of $m_{\rm W}$ from UA2 [72], CDF [73, 74], and DØ [75][3], measurements of the top quark mass by CDF [77] and DØ [78][4], and measurements of the neutrino-nucleon neutral to charged current ratios from CCFR [80] and NuTeV [81]. Although the $\nu\mathcal{N}$ results are quoted in terms of $\sin^2\theta_W = 1 - m_{\rm W}^2/m_{\rm Z}^2$, radiative corrections result in small $m_{\rm t}$ and $m_{\rm H}$ dependences[5] that are included in the fit. An additional input parameter, not shown in the table, is the Fermi constant G_F, determined from the μ lifetime, $G_F = (1.16637 \pm 0.00001) \times 10^{-5}\text{GeV}^{-2}$ [82]. The relative error of G_F is comparable to that of $m_{\rm Z}$; both errors have negligible effects in the fit results.

12.5.2 Uncertainties

Detailed studies of the theoretical uncertainties in the Standard Model predictions due to missing higher-order electroweak corrections and their interplay with QCD corrections have been carried out in the working group on 'Precision calculations for the Z resonance' [84], and more recently in [15]. Theoretical uncertainties are evaluated by comparing different but, within our present knowledge, equivalent treatments of aspects such as resummation techniques, momentum transfer scales for vertex corrections and factorisation schemes. The effects of these theoretical uncertainties have been reduced by the inclusion of higher-order corrections [85, 86] in the electroweak libraries [87]. The very recently calculated complete fermionic two-loop calculations for $m_{\rm W}$ [88] are not yet included as the effect on $m_{\rm W}$ is small compared to the current experimental uncertainty on $m_{\rm W}$ and the corresponding calculations of the effective weak mixing angle and the partial Z widths are not yet available. The use of the new QCD corrections [86] increases the value of $\alpha_{\rm s}(m_{\rm Z}^2)$ by 0.001, as expected. The effects of missing higher-order QCD corrections on $\alpha_{\rm s}(m_{\rm Z}^2)$ covers missing higher-order electroweak corrections and uncertainties in the interplay of electroweak and QCD corrections and is estimated to be at least 0.002 [89]. A discussion of theoretical uncertainties in the determination of $\alpha_{\rm s}$ can be found in References 84 and 89. The determination of the size of remaining theoretical uncertainties is under continued study. The theoretical errors discussed in this paragraph are not included in the results presented in Table 18.

At present the impact of theoretical uncertainties on the determination of SM parameters from the precise electroweak measurements is small compared to the error due to the uncertainty in the

[3] See Reference 76 for a combination of these $m_{\rm W}$ measurements.
[4] See Reference 79 for a combination of these $m_{\rm t}$ measurements.
[5] The formula used is $\delta\sin^2\theta_W = -0.00142\,\frac{m_{\rm t}^2-(175\text{GeV})^2}{(100\text{GeV})^2} + 0.00048\,\ln(\frac{m_{\rm H}}{150\text{GeV}})$. See Reference 81 for details.

	Measurement with Total Error	Systematic Error	Standard Model fit	Pull
$\Delta\alpha^{(5)}_{\rm had}(m_{\rm Z}^2)$ [83]	0.02761 ± 0.00036	0.00035	0.02774	-0.4
a) LEP				
line-shape and				
lepton asymmetries:				
$m_{\rm Z}$ [GeV]	91.1875 ± 0.0021	[a]0.0017	91.1874	0.0
$\Gamma_{\rm Z}$ [GeV]	2.4952 ± 0.0023	[a]0.0012	2.4962	-0.5
$\sigma^0_{\rm h}$ [nb]	41.540 ± 0.037	[b]0.028	41.480	1.6
R_ℓ	20.767 ± 0.025	[b]0.007	20.740	1.1
$A^{0,\ell}_{\rm FB}$	0.0171 ± 0.0010	[b]0.0003	0.0164	0.8
+ correlation matrix Table 3				
τ polarisation:				
$\mathcal{A}_\tau$	0.1439 ± 0.0041	0.0022	0.1478	-1.0
$\mathcal{A}_{\rm e}$	0.1498 ± 0.0048	0.0008	0.1478	0.4
$q\overline{q}$ charge asymmetry:				
$\sin^2\theta^{\rm lept}_{\rm eff}$ ($\langle Q_{\rm FB}\rangle$)	0.2322 ± 0.0010	0.0008	0.23142	0.8
$m_{\rm W}$ [GeV]	80.446 ± 0.040	0.030	80.393	1.3
b) SLD [70]				
$\mathcal{A}_\ell$ (SLD)	0.1513 ± 0.0021	0.0010	0.1478	1.7
c) LEP and SLD Heavy Flavour				
$R^0_{\rm b}$	0.21664 ± 0.00068	0.00053	0.21574	1.3
$R^0_{\rm c}$	0.1729 ± 0.0032	0.0022	0.1723	0.2
$A^{0,{\rm b}}_{\rm FB}$	0.0982 ± 0.0017	0.0009	0.1036	-3.1
$A^{0,{\rm c}}_{\rm FB}$	0.0689 ± 0.0035	0.0017	0.0741	-1.5
$\mathcal{A}_{\rm b}$	0.921 ± 0.020	0.016	0.935	-0.7
$\mathcal{A}_{\rm c}$	0.667 ± 0.026	0.016	0.668	-0.0
+ correlation matrix Table 10				
d) $p\overline{p}$ and νN				
$m_{\rm W}$ [GeV] ($p\overline{p}$ [76])	80.452 ± 0.062	0.050	80.393	0.9
$1 - m^2_{\rm W}/m^2_{\rm Z}$ (νN [80,81])	0.2255 ± 0.0021	0.0010	0.2227	1.2
$m_{\rm t}$ [GeV] ($p\overline{p}$ [79])	174.3 ± 5.1	4.0	175.7	-0.3

Table 17: Summary of measurements included in the combined analysis of Standard Model parameters. Section a) summarises LEP averages, Section b) SLD results ($\sin^2\theta^{\rm lept}_{\rm eff}$ includes $A_{\rm LR}$ and the polarised lepton asymmetries), Section c) the LEP and SLD heavy flavour results and Section d) electroweak measurements from $p\overline{p}$ colliders and νN scattering. The total errors in column 2 include the systematic errors listed in column 3. Although the systematic errors include both correlated and uncorrelated sources, the determination of the systematic part of each error is approximate. The Standard Model results in column 4 and the pulls (difference between measurement and fit in units of the total measurement error) in column 5 are derived from the Standard Model fit including all data (Table 18, column 5) with the Higgs mass treated as a free parameter.

[a] The systematic errors on $m_{\rm Z}$ and $\Gamma_{\rm Z}$ contain the errors arising from the uncertainties in the LEP energy only.

[b] Only common systematic errors are indicated.

value of $\alpha(m_{\rm Z}^2)$. The uncertainty in $\alpha(m_{\rm Z}^2)$ arises from the contribution of light quarks to the photon vacuum polarisation ($\Delta\alpha^{(5)}_{\rm had}(m_{\rm Z}^2)$):

$$\alpha(m_{\rm Z}^2) = \frac{\alpha(0)}{1 - \Delta\alpha_\ell(m_{\rm Z}^2) - \Delta\alpha^{(5)}_{\rm had}(m_{\rm Z}^2) - \Delta\alpha_{\rm top}(m_{\rm Z}^2)}\,, \tag{27}$$

where $\alpha(0) = 1/137.036$. The top contribution, $-0.00007(1)$, depends on the mass of the top quark, and is therefore determined inside the electroweak libraries [87]. The leptonic contribution is calculated to third order [90] to be 0.03150, with negligible uncertainty.

For the hadronic contribution, we no longer use the value 0.02804 ± 0.00065 [91], but rather the new evaluation 0.02761 ± 0.0036 [83] which takes into account the recently published results on electron-positron annihilations into hadrons at low centre-of-mass energies by the BES collaboration [92]. This reduced uncertainty still causes an error of 0.00013 on the Standard Model prediction of $\sin^2\theta^{\rm lept}_{\rm eff}$, and errors of 0.2 GeV and 0.1 on the fitted values of $m_{\rm t}$ and $\log(m_{\rm H})$, all included in the results. The effect on the Standard Model prediction for $\Gamma_{\ell\ell}$ is negligible. The $\alpha_{\rm s}(m_{\rm Z}^2)$ values for the Standard Model fits presented in this Section are stable against a variation of $\alpha(m_{\rm Z}^2)$ in the interval quoted. There are also several evaluations of $\Delta\alpha^{(5)}_{\rm had}(m_{\rm Z}^2)$ [93–100] which are more theory driven. The most recent of these (Reference 99) also includes the new results from BES, 0.02738 ± 0.00020. To show the effects of the uncertainty of $\alpha(m_{\rm Z}^2)$, we also use this evaluation of the hadronic vacuum polarisation. Note that all these evaluations obtain values for $\Delta\alpha^{(5)}_{\rm had}(m_{\rm Z}^2)$ consistently lower than - but still in agreement with - the old value of 0.02804 ± 0.00065.

12.5.3 Results

Figure 7 shows a comparison of the leptonic partial width from LEP (Table 4) and the effective electroweak mixing angle from asymmetries measured at LEP and SLD (Table 16), with the Standard Model. Good agreement with the Standard Model prediction is observed. The point with the arrow shows the prediction if among the electroweak radiative corrections only the photon vacuum polarisation is included, which shows an example of evidence that LEP+SLD data are sensitive to electroweak corrections. Note that the error due to the uncertainty on $\alpha(m_{\rm Z}^2)$ (shown as the length of the arrow) is not much smaller than the experimental error on $\sin^2\theta^{\rm lept}_{\rm eff}$ from LEP and SLD. This underlines the continued importance of a precise measurement of $\sigma(e^+e^- \to \text{hadrons})$ at low centre-of-mass energies.

Of the measurements given in Table 17, R_ℓ is one of the most sensitive to QCD corrections. For $m_{\rm Z} = 91.1875$ GeV, and imposing $m_{\rm t} = 174.3 \pm 5.1$ GeV as a constraint, $\alpha_{\rm s} = 0.122 \pm 0.004$ is obtained. Alternatively, σ^0_ℓ (see Table 4) which has higher sensitivity to QCD corrections and less dependence on $m_{\rm H}$ yields: $\alpha_{\rm s} = 0.118 \pm 0.003$. Typical errors arising from variation $m_{\rm H}$ are of the order of 0.001, somewhat smaller for σ^0_ℓ. These results are in very good agreement with the world average ($\alpha_{\rm s}(m_{\rm Z}^2) = 0.118 \pm 0.002$ [101]).

12.5.4 Standard-Model Fits

In the following, several different fits to the data in the framework of the Standard-Model as reported in Table 18 are discussed. The large χ^2/d.o.f. for all of these fits is caused by the very same effect as discussed in the previous Sections, namely the large dispersion in the values of the leptonic effective electroweak mixing angle measured through the various asymmetries. For the analyses presented here,

this dispersion is interpreted as a fluctuation in one or more of the input measurements, and thus we neither modify nor exclude any of them.

To test the agreement between the LEP data and the Standard Model, a fit to the data (including the LEP-II $m_{\rm W}$ determination) leaving the top quark mass and the Higgs mass as free parameters is performed. The result is shown in Table 18, column 1. This fit shows that the LEP data prefer a light top quark and a light Higgs boson, albeit with very large errors. The strongly asymmetric errors on $m_{\rm H}$ are due to the fact that to first order, the radiative corrections in the Standard Model are proportional to $\log(m_{\rm H})$.

The data can also be used within the Standard Model to determine the top quark and W masses indirectly, which can be compared to the direct measurements performed at the $\rm p\overline{p}$ colliders and LEP. In the second fit, all the results in Table 17, except the LEP-II and $\rm p\overline{p}$ colliders $m_{\rm W}$ and $m_{\rm t}$ results are used. The results are shown in column 2 of Table 18. The indirect measurements of $m_{\rm W}$ and $m_{\rm t}$ from this data sample are shown in Figure 8, compared with the direct measurements. Also shown is the Standard Model predictions for Higgs masses between 113 and 1000 GeV. As can be seen in the figure, the indirect and direct measurements of $m_{\rm W}$ and $m_{\rm t}$ are in good agreement, and both sets prefer a low value of the Higgs mass.

For the third fit, the direct $m_{\rm t}$ measurement is used to obtain the best indirect determination of $m_{\rm W}$. The result is shown in column 3 of Table 18 and in Figure 9. Also here, the indirect determination of W boson mass 80.368 ± 0.023 GeV is in agreement with the combination of direct measurements from LEP-2 and $\rm p\overline{p}$ colliders [76] of $m_{\rm W} = 80.448 \pm 0.034$ GeV. For the next fit, (column 4 of Table 18 and Figure 10), the direct $m_{\rm W}$ measurements from LEP and $\rm p\overline{p}$ colliders are included to obtain $m_{\rm t} = 180^{+12}_{-9}$ GeV, in very good agreement with the direct measurement of $m_{\rm t} = 174.3 \pm 5.1$ GeV.

Finally, the best constraints on $m_{\rm H}$ are obtained when all data are used in the fit. The results of this fit are shown in column 5 of Table 18 and in Figure 10. In Figures 11 and 12 the sensitivity of the LEP and SLD measurements to the Higgs mass is shown. As can be seen, the most sensitive measurements are the asymmetries. A reduced uncertainty for the value of $\alpha(m_{\rm Z}^2)$ would therefore result in an improved constraint on $m_{\rm H}$, as shown in Figures 7 and 13.

In Figure 13 the observed value of $\Delta\chi^2 \equiv \chi^2 - \chi^2_{\rm min}$ as a function of $m_{\rm H}$ is plotted for the fit including all data. The solid curve is the result using ZFITTER, and corresponds to the last column of Table 18. The shaded band represents the uncertainty due to uncalculated higher-order corrections, as estimated by ZFITTER and TOPAZ0. The 95% confidence level upper limit on $m_{\rm H}$ (taking the band into account) is 212 GeV. The lower limit on $m_{\rm H}$ of approximately 113 GeV obtained from direct searches [102] has not been used in the determination of this limit. Also shown is the result (dashed curve) obtained when using $\Delta\alpha^{(5)}_{\rm had}(m_{\rm Z}^2)$ of Reference 99. That fit results in $\log(m_{\rm H}/{\rm GeV}) = 2.07 \pm 0.19$ corresponding to $m_{\rm H} = 118^{+63}_{-42}$ GeV and an upper limit on $m_{\rm H}$ of approximately 236 GeVat 95% confidence level.

	- 1 - LEP including LEP-II $m_{\rm W}$	- 2 - all data except $m_{\rm W}$ and $m_{\rm t}$	- 3 - all data except $m_{\rm W}$	- 4 - all data except $m_{\rm t}$	- 5 - all data
$m_{\rm t}$ [GeV]	187^{+13}_{-12}	168^{+12}_{-9}	$173.3^{+4.8}_{-4.7}$	180^{+12}_{-9}	$175.7^{+4.4}_{-4.3}$
$m_{\rm H}$ [GeV]	311^{+494}_{-187}	87^{+119}_{-43}	121^{+76}_{-48}	139^{+203}_{-77}	98^{+58}_{-38}
$\log(m_{\rm H}/{\rm GeV})$	$2.49^{+0.41}_{-0.40}$	$1.94^{+0.37}_{-0.30}$	$2.08^{+0.21}_{-0.22}$	$2.14^{+0.39}_{-0.35}$	$1.99^{+0.20}_{-0.21}$
$\alpha_{\rm s}(m_{\rm Z}^2)$	0.121 ± 0.003	0.119 ± 0.003	0.119 ± 0.003	0.119 ± 0.003	0.118 ± 0.003
χ^2/d.o.f.	17/9	21/12	22/13	25/14	26/15
$\sin^2\theta^{\rm lept}_{\rm eff}$	0.23168	0.23155	0.23156	0.23144	0.23142
	± 0.00017	± 0.00016	± 0.00016	± 0.00015	± 0.00014
$1 - m_{\rm W}^2/m_{\rm Z}^2$	0.22292	0.22344	0.22232	0.22259	0.22273
	± 0.00051	± 0.00063	± 0.00045	± 0.00045	± 0.00036
$m_{\rm W}$ [GeV]	80.384 ± 0.027	80.357 ± 0.033	80.368 ± 0.023	80.401 ± 0.023	80.393 ± 0.019

Table 18: Results of the fits to LEP data alone, to all data except the direct determinations of $m_{\rm t}$ and $m_{\rm W}$ ($\rm p\overline{p}$ collider and LEP-II), to all data except direct $m_{\rm W}$ determinations, and to all data. As the sensitivity to $m_{\rm H}$ is logarithmic, both $m_{\rm H}$ as well as $\log(m_{\rm H}/{\rm GeV})$ are quoted. The bottom part of the table lists derived results for $\sin^2\theta^{\rm lept}_{\rm eff}$, $1 - m_{\rm W}^2/m_{\rm Z}^2$ and $m_{\rm W}$. See text for a discussion of theoretical errors not included in the errors above.

13 Prospects for the Future

Most of the measurements from data taken at or near the Z resonance, both at LEP as well as at SLC, that are presented in this report are either final or are being finalised. The major improvements will therefore take place in the high energy data. With more than 600 pb^{-1} per experiment, LEP-II will lead to substantially improved measurements of certain electroweak parameters. The measurements of m_{W} are likely to match the error obtained via the radiative corrections of the Z data, providing a further important test of the Standard Model. In the measurement of the WWγ and WWZ triple-gauge-boson couplings the increase in LEP-II statistics, together with the increased sensitivity at higher beam energies, will lead to an improvement in the current precision.

14 Conclusions

The combination of the many precise electroweak results yields stringent constraints on the Standard Model. In addition, the results are sensitive to the Higgs mass. Most measurements agree well with the predictions. The spread in values of the various determinations of the effective electroweak mixing angle is larger than expected. Within the Standard Model analysis, this seems to be caused by the measurement of the forward-backward asymmetry in b-quark production, showing the largest deviation w.r.t. the Standard-Model expectation.

The experiments wish to stress that this report reflects a preliminary status at the time of the 2001 winter conferences. A definitive statement on these results must wait for publication by each collaboration.

Acknowledgements

We would like to thank the CERN accelerator divisions for the efficient operation of the LEP accelerator, the precise information on the absolute energy scale and their close cooperation with the four experiments. The SLD collaboration would like to thank the SLAC accelerator department for the efficient operation of the SLC accelerator. We would also like to thank members of the CDF, DØ and NuTeV Collaborations for making results available to us in advance of the conferences and for useful discussions concerning their combination. Finally, the results of the section on Standard Model constraints would not have been possible without the close collaboration of many theorists.

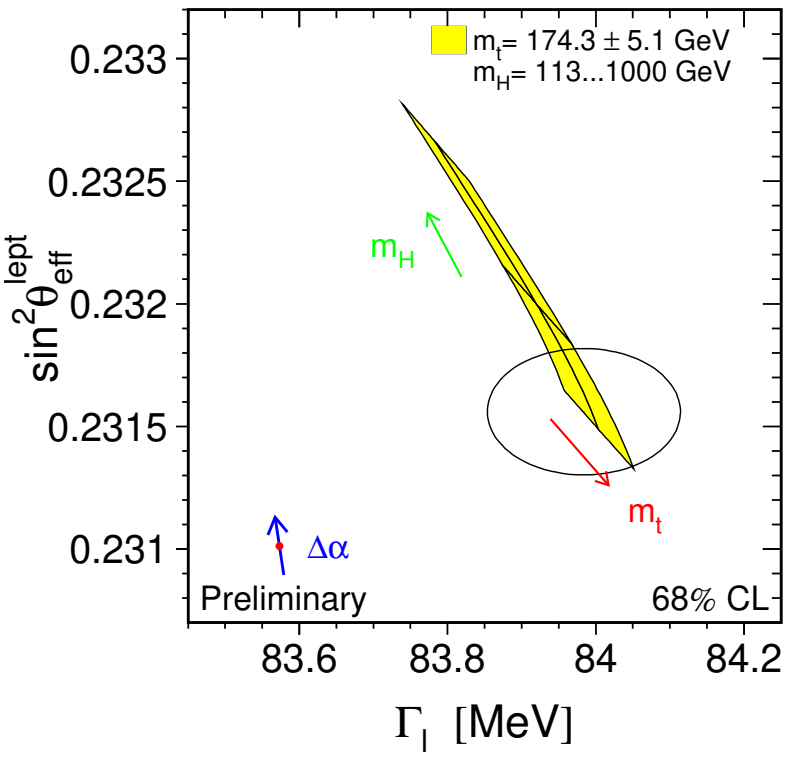

Figure 7: LEP-I+SLD measurements of $\sin^2\theta^{\mathrm{lept}}_{\mathrm{eff}}$ (Table 16) and $\Gamma_{\ell\ell}$ (Table 4) and the Standard Model prediction. The point shows the predictions if among the electroweak radiative corrections only the photon vacuum polarisation is included. The corresponding arrow shows variation of this prediction if $\alpha(m_{\mathrm{Z}}^2)$ is changed by one standard deviation. This variation gives an additional uncertainty to the Standard Model prediction shown in the figure.

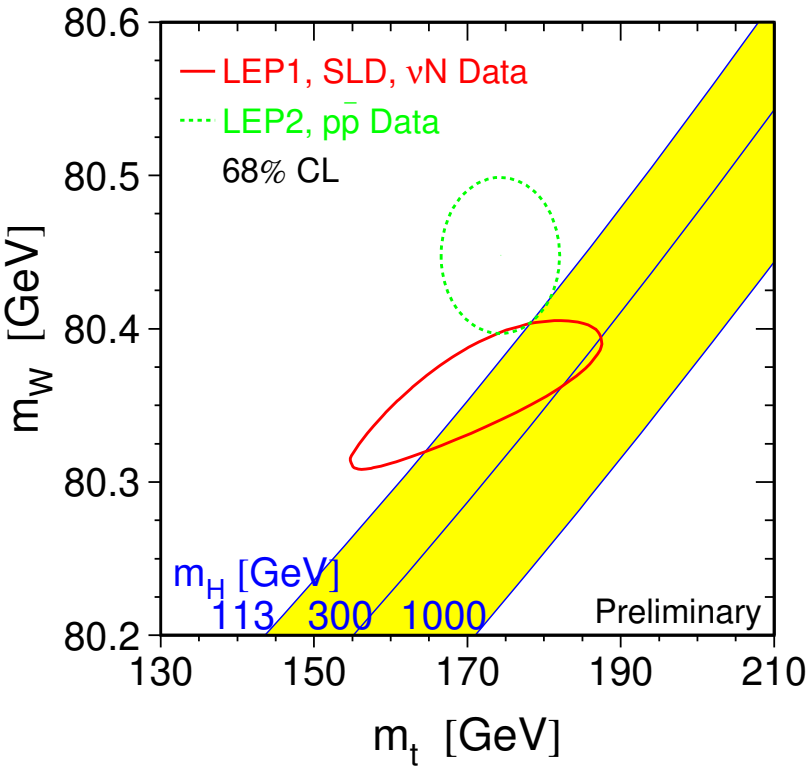

Figure 8: The comparison of the indirect measurements of m_{W} and m_{t} (LEP-I+SLD+νN data) (solid contour) and the direct measurements ($\mathrm{p\overline{p}}$ colliders and LEP-II data) (dashed contour). In both cases the 68% CL contours are plotted. Also shown is the Standard Model relationship for the masses as a function of the Higgs mass.

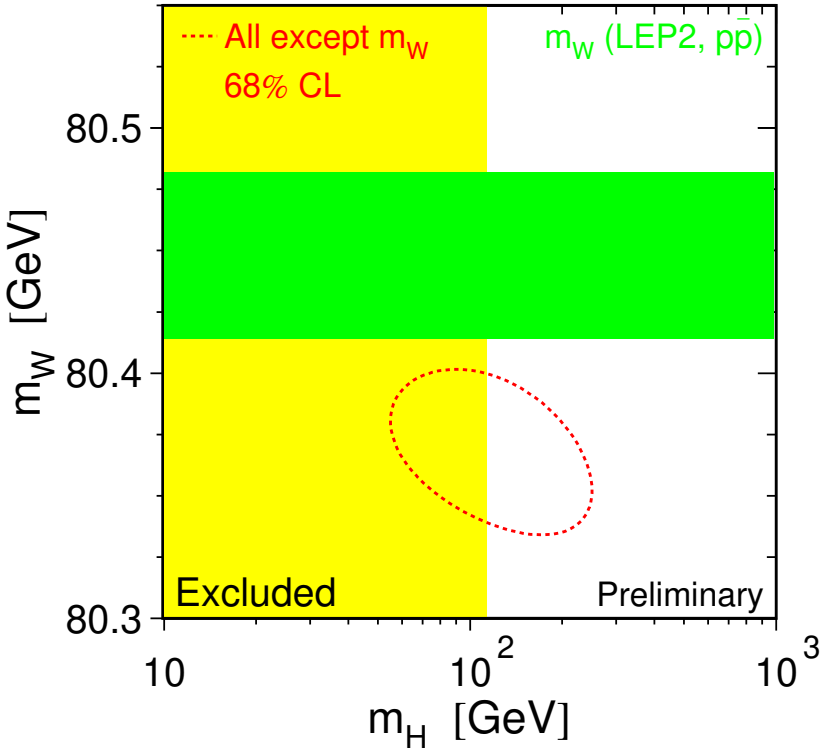

Figure 9: The 68% confidence level contour in m_{t} and m_{W} for the fit to all data except the direct measurement of m_{W}, indicated by the shaded horizontal band of ± 1 sigma width. The vertical band shows the 95% CL exclusion limit on m_{H} from the direct search.

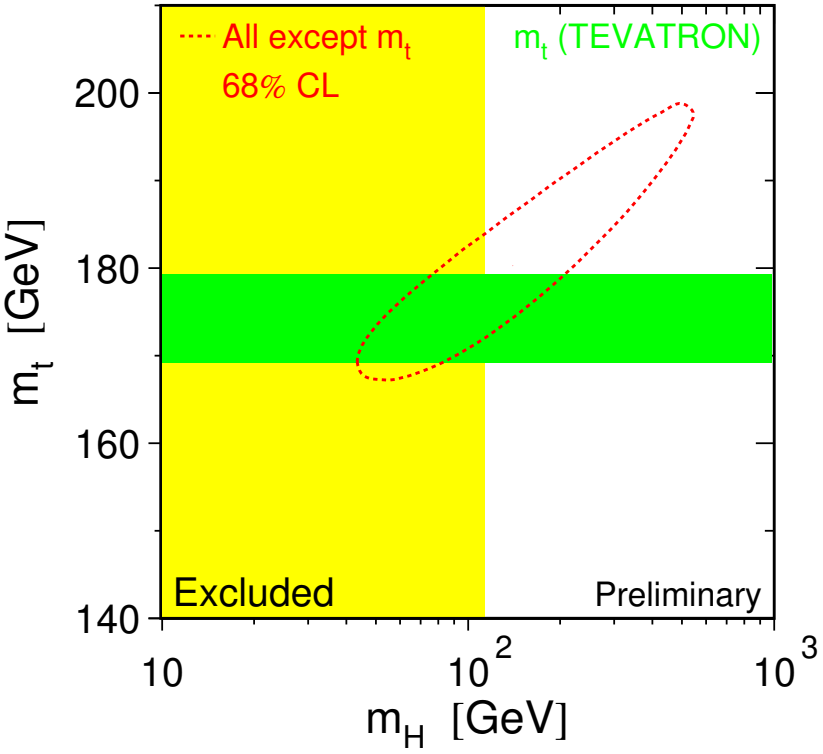

Figure 10: The 68% confidence level contour in $m_{\rm t}$ and $m_{\rm H}$ for the fit to all data except the direct measurement of $m_{\rm t}$, indicated by the shaded horizontal band of ± 1 sigma width. The vertical band shows the 95% CL exclusion limit on $m_{\rm H}$ from the direct search.

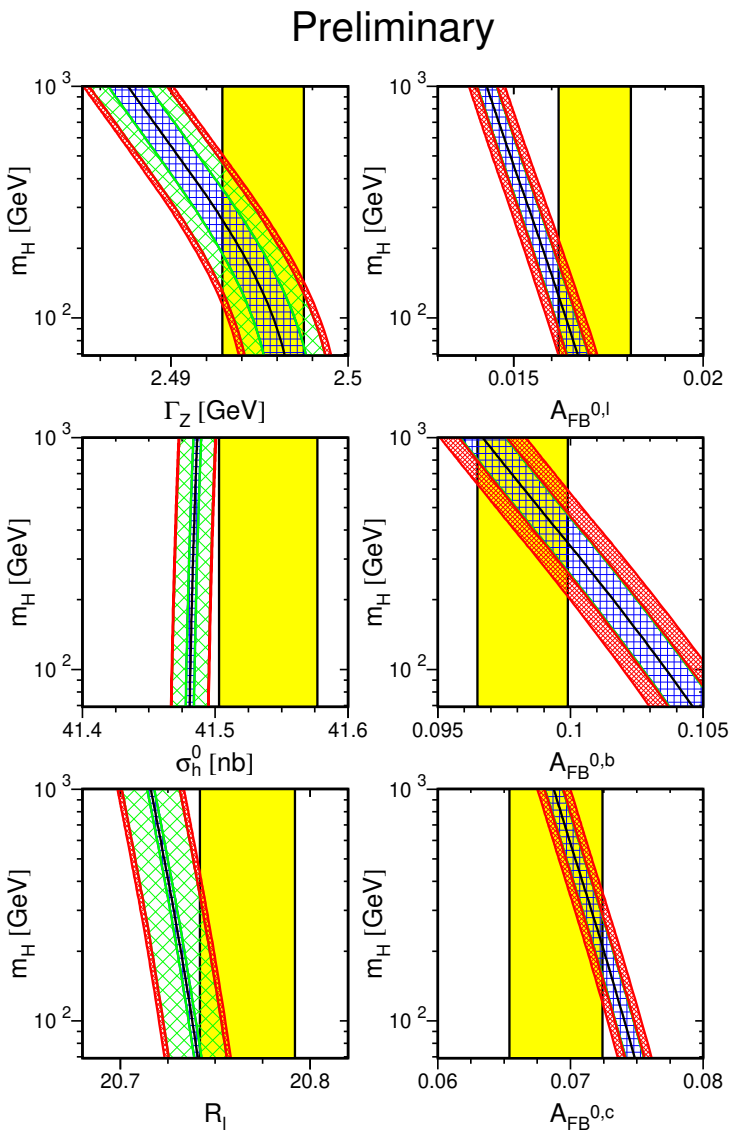

Figure 11: Comparison of LEP-I measurements with the Standard Model prediction as a function of $m_{\rm H}$. The measurement with its error is shown as the vertical band. The width of the Standard Model band is due to the uncertainties in $\Delta\alpha^{(5)}_{\rm had}(m^2_{\rm Z})$, $\alpha_{\rm s}(m^2_{\rm Z})$ and $m_{\rm t}$. The total width of the band is the linear sum of these effects. See Figure 12 for the definition of these uncertainties.

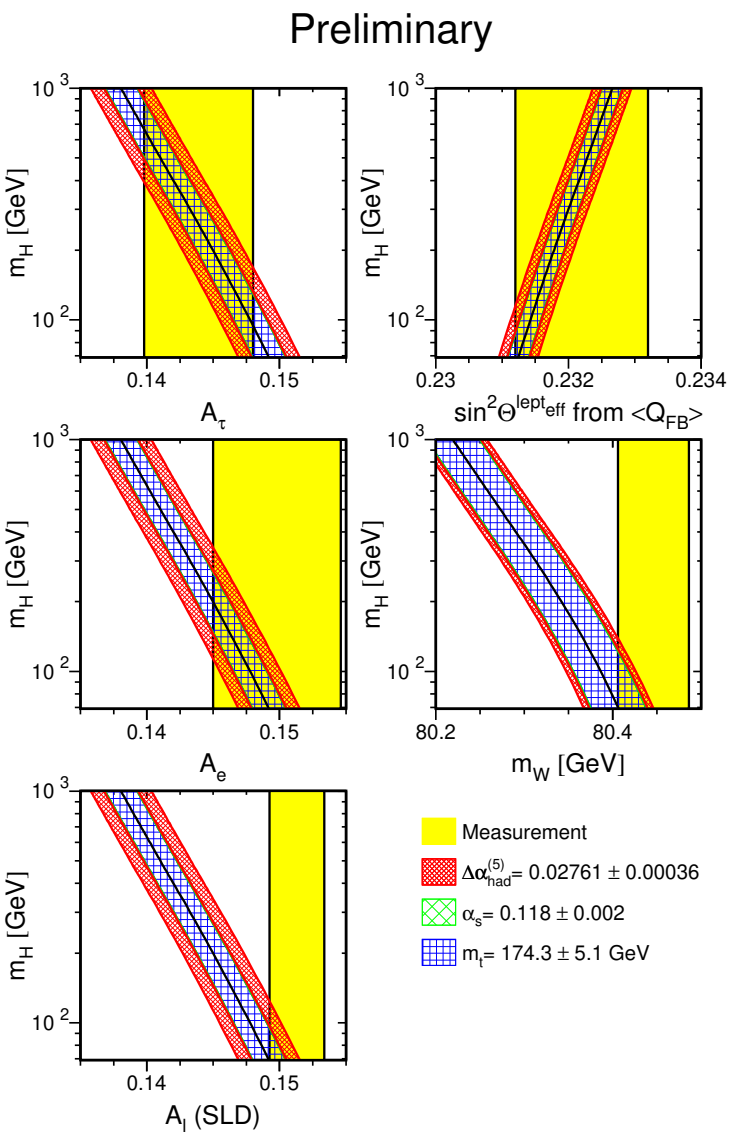

Figure 12: Comparison of LEP-I measurements with the Standard Model prediction as a function of $m_{\rm H}$ (*c.f.* Figure 11). Also shown is the comparison of the SLD measurement of $A^0_{\rm LR}$ with the Standard Model.

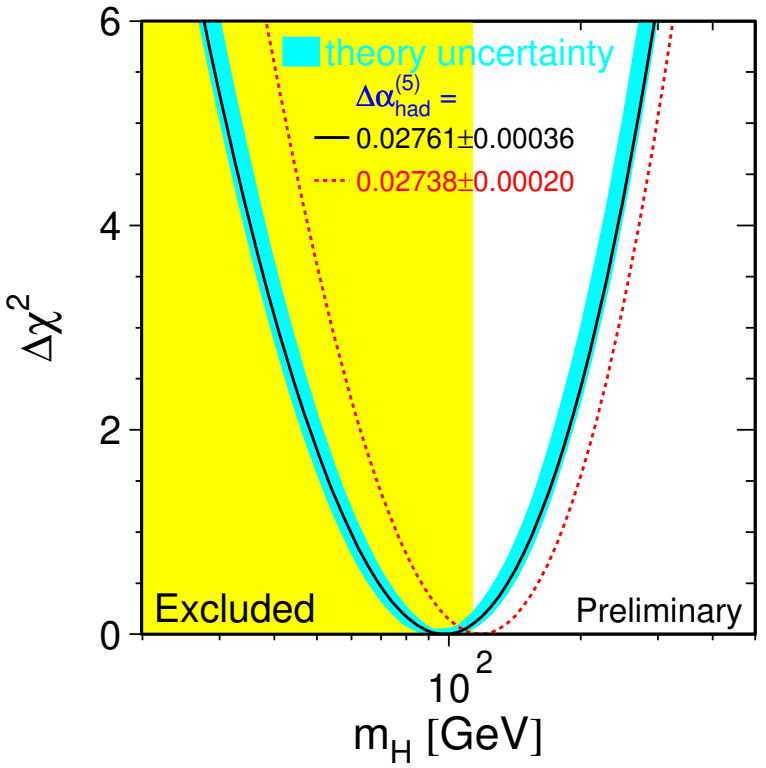

Figure 13: $\Delta\chi^2 = \chi^2 - \chi^2_{min}$ *vs.* $m_{\rm H}$ curve. The line is the result of the fit using all data (last column of Table 18); the band represents an estimate of the theoretical error due to missing higher order corrections. The vertical band shows the 95% CL exclusion limit on $m_{\rm H}$ from the direct search. The dashed curve is the result obtained using the evaluation of $\Delta\alpha^{(5)}_{\rm had}(m^2_{\rm Z})$ from Reference 99.

Appendix

A Heavy-Flavour Fit including Off-Peak Asymmetries

The full 18 parameter fit to the LEP and SLD data gave the following results:

$$
\begin{aligned}
R_{\mathrm{b}}^{0} &= 0.21664 \pm 0.00068 \\
R_{\mathrm{c}}^{0} &= 0.1729 \pm 0.0032 \\
A_{\mathrm{FB}}^{\mathrm{b\bar{b}}}(-2) &= 0.0521 \pm 0.0069 \\
A_{\mathrm{FB}}^{\mathrm{c\bar{c}}}(-2) &= -0.026 \pm 0.015 \\
A_{\mathrm{FB}}^{\mathrm{b\bar{b}}}(\mathrm{pk}) &= 0.0964 \pm 0.0018 \\
A_{\mathrm{FB}}^{\mathrm{c\bar{c}}}(\mathrm{pk}) &= 0.0621 \pm 0.0036 \\
A_{\mathrm{FB}}^{\mathrm{b\bar{b}}}(+2) &= 0.1150 \pm 0.0058 \\
A_{\mathrm{FB}}^{\mathrm{c\bar{c}}}(+2) &= 0.131 \pm 0.013 \\
\mathcal{A}_{\mathrm{b}} &= 0.921 \pm 0.020 \\
\mathcal{A}_{\mathrm{c}} &= 0.667 \pm 0.026 \\
\mathrm{BR}(\mathrm{b} \to \ell) &= 0.1057 \pm 0.0019 \\
\mathrm{BR}(\mathrm{b} \to \mathrm{c} \to \bar{\ell}) &= 0.0801 \pm 0.0020 \\
\mathrm{BR}(\mathrm{c} \to \ell) &= 0.0974 \pm 0.0032 \\
\overline{\chi} &= 0.1192 \pm 0.0043 \\
f(\mathrm{D}^{+}) &= 0.233 \pm 0.016 \\
f(\mathrm{D_s}) &= 0.130 \pm 0.027 \\
f(\mathrm{c_{baryon}}) &= 0.096 \pm 0.023 \\
\mathrm{P}(\mathrm{c} \to \mathrm{D}^{*+}) \times \mathrm{BR}(\mathrm{D}^{*+} \to \pi^{+}\mathrm{D}^{0}) &= 0.1608 \pm 0.0048
\end{aligned}
$$

with a χ^2/d.o.f. of $48/(99-18)$. The corresponding correlation matrix is given in Table 19. The energy for the peak−2, peak and peak+2 results are respectively 89.55 GeV, 91.26 GeV and 92.94 GeV. Note that the asymmetry results shown here are not the pole asymmetries shown in Section 5.2.2. The non-electroweak parameters do not depend on the treatment of the asymmetries.

	1) R_{b}	2) R_{c}	3) $A_{\mathrm{FB}}^{\mathrm{b\bar{b}}}(-2)$	4) $A_{\mathrm{FB}}^{\mathrm{c\bar{c}}}(-2)$	5) $A_{\mathrm{FB}}^{\mathrm{b\bar{b}}}(\mathrm{pk})$	6) $A_{\mathrm{FB}}^{\mathrm{c\bar{c}}}(\mathrm{pk})$	7) $A_{\mathrm{FB}}^{\mathrm{b\bar{b}}}(+2)$	8) $A_{\mathrm{FB}}^{\mathrm{c\bar{c}}}(+2)$	9) $\mathcal{A}_{\mathrm{b}}$	10) $\mathcal{A}_{\mathrm{c}}$	11) BR (1)	12) BR (2)	13) BR (3)	14) $\overline{\chi}$	15) $f(\mathrm{D}^{+})$	16) $f(\mathrm{D_s})$	17) $f(\mathrm{c_{bar.}})$	18) PcDst
1)	1.00	−0.16	−0.02	0.00	−0.08	0.01	−0.03	0.00	−0.06	0.02	−0.08	−0.01	−0.02	−0.03	−0.15	−0.04	0.12	0.13
2)	−0.16	1.00	0.01	0.01	0.04	−0.02	0.01	−0.01	0.03	−0.04	0.04	0.00	−0.30	0.03	−0.11	0.18	0.14	−0.44
3)	−0.02	0.01	1.00	0.16	0.03	0.01	0.01	0.00	0.01	0.00	0.02	−0.03	0.01	0.05	0.00	0.00	0.00	0.00
4)	0.00	0.01	0.16	1.00	0.01	0.02	0.00	0.00	0.00	0.00	0.01	−0.01	0.02	0.01	0.00	0.00	0.00	0.01
5)	−0.08	0.04	0.03	0.01	1.00	0.16	0.08	0.01	0.02	0.00	0.03	−0.08	0.01	0.14	0.03	0.05	−0.04	−0.02
6)	0.01	−0.02	0.01	0.02	0.16	1.00	0.01	0.09	0.00	0.01	0.14	−0.17	−0.05	0.17	0.00	0.00	−0.01	0.01
7)	−0.03	0.01	0.01	0.00	0.08	0.01	1.00	0.17	0.01	0.00	0.00	−0.02	0.01	0.06	0.01	0.01	−0.01	−0.01
8)	0.00	−0.01	0.00	0.00	0.01	0.09	0.17	1.00	0.00	0.00	0.02	−0.04	−0.03	0.02	0.00	−0.01	0.00	0.01
9)	−0.06	0.03	0.01	0.00	0.02	0.00	0.01	0.00	1.00	0.12	−0.02	0.00	0.05	0.07	0.00	0.00	0.00	−0.02
10)	0.02	−0.04	0.00	0.00	0.00	0.01	0.00	0.00	0.12	1.00	0.02	−0.03	−0.03	0.00	0.00	0.00	0.00	0.01
11)	−0.08	0.04	0.02	0.01	0.03	0.14	0.00	0.02	−0.02	0.02	1.00	−0.33	0.15	0.43	0.04	0.01	−0.02	−0.02
12)	−0.01	0.00	−0.03	−0.01	−0.08	−0.17	−0.02	−0.04	0.00	−0.03	−0.33	1.00	−0.03	−0.40	0.01	−0.01	0.00	0.00
13)	−0.02	−0.30	0.01	0.02	0.01	−0.05	0.01	−0.03	0.05	−0.03	0.15	−0.03	1.00	0.21	0.01	−0.03	−0.02	0.13
14)	−0.03	0.03	0.05	0.01	0.14	0.17	0.06	0.02	0.07	0.00	0.43	−0.40	0.21	1.00	0.02	0.02	−0.01	−0.02
15)	−0.15	−0.11	0.00	0.00	0.03	0.00	0.01	0.00	0.00	0.00	0.04	0.01	0.01	0.02	1.00	−0.40	−0.24	0.09
16)	−0.04	0.18	0.00	0.00	0.05	0.00	0.01	−0.01	0.00	0.00	0.01	−0.01	−0.03	0.02	−0.40	1.00	−0.52	−0.09
17)	0.12	0.14	0.00	0.00	−0.04	−0.01	−0.01	0.00	0.00	0.00	−0.02	0.00	−0.02	−0.01	−0.24	−0.52	1.00	−0.13
18)	0.13	−0.44	0.00	0.01	−0.02	0.01	−0.01	0.01	−0.02	0.01	−0.02	0.00	0.13	−0.02	0.09	−0.09	−0.13	1.00

Table 19: The correlation matrix for the set of the 18 heavy flavour parameters. BR(1), BR(2) and BR(3) denote $\mathrm{BR}(\mathrm{b} \to \ell)$, $\mathrm{BR}(\mathrm{b} \to \mathrm{c} \to \bar{\ell})$ and $\mathrm{BR}(\mathrm{c} \to \ell)$ respectively, PcDst denotes $\mathrm{P}(\mathrm{c} \to \mathrm{D}^{*+}) \times \mathrm{BR}(\mathrm{D}^{*+} \to \pi^{+}\mathrm{D}^{0})$.

The Measurements used in the Heavy Flavour Averages

In the following 20 tables the results used in the combination are listed. In each case an indication of the dataset used and the type of analysis is given. Preliminary results are indicated by the symbol "†". The values of centre-of-mass energy are given where relevant. In each table, the result used as input to the average procedure is given followed by the statistical error, the correlated and uncorrelated systematic errors, the total systematic error, and any dependence on other electroweak parameters. In the case of the asymmetries, the measurement moved to a common energy (89.55 GeV, 91.26 GeV and 92.94 GeV, respectively, for peak−2, peak and peak+2 results) is quoted as *corrected* asymmetry.

Contributions to the correlated systematic error quoted here are from any sources of error shared with one or more other results from different experiments in the same table, and the uncorrelated errors from the remaining sources. In the case of $\mathcal{A}_c$ and $\mathcal{A}_b$ from SLD the quoted correlated systematic error has contributions from any source shared with one or more other measurements from LEP experiments. Constants such as $a(x)$ denote the dependence on the assumed value of x^{used}, which is also given.

	ALEPH	DELPHI	L3	OPAL	SLD
	92-95	92-95	94-95	92-95	93-98†
	[25]	[26]	[27]	[28]	[29]
R_b	0.2157	0.2163	0.2174	0.2174	0.2171
Statistical	0.0009	0.0007	0.0015	0.0011	0.0009
Uncorrelated	0.0007	0.0004	0.0015	0.0009	0.0005
Correlated	0.0007	0.0004	0.0018	0.0008	0.0005
Total Systematic	0.0009	0.0006	0.0023	0.0012	0.0008
$a(R_c)$	-0.0033	-0.0041	-0.0376	-0.0122	-0.0057
R_c^{used}	0.1720	0.1720	0.1734	0.1720	0.1710
$a(\text{BR}(c \to \ell))$			-0.0133	-0.0067	
$\text{BR}(c \to \ell)^{\text{used}}$			9.80	9.80	
$a(f(D^+))$	-0.0010	-0.0010	-0.0086	-0.0029	-0.0008
$f(D^+)^{\text{used}}$	0.2330	0.2330	0.2330	0.2380	0.2370
$a(f(D_s))$	-0.0001	0.0001	-0.0005	-0.0001	-0.0003
$f(D_s)^{\text{used}}$	0.1020	0.1030	0.1030	0.1020	0.1140
$a(f(\Lambda_c))$	0.0002	0.0003	0.0008	0.0003	-0.0003
$f(\Lambda_c)^{\text{used}}$	0.0650	0.0630	0.0630	0.0650	0.0730

Table 20: The measurements of R_b. All measurements use a lifetime tag enhanced by other features like invariant mass cuts or high p_T leptons.

	ALEPH			DELPHI		OPAL		SLD
	91-95	91-95	92-95	92-95	92-95	91-94	90-95	93-97†
	c-count	D meson	lepton	c-count	D meson	c-count	D meson	vtx-mass
	[34]	[30]	[30]	[32]	[32]	[35]	[33]	[29]
R_c	0.1734	0.1679	0.1668	0.1692	0.1610	0.164	0.1760	0.1754
Statistical	0.0049	0.0082	0.0062	0.0047	0.0104	0.011	0.0095	0.0032
Uncorrelated	0.0057	0.0078	0.0059	0.0050	0.0064	0.012	0.0102	0.0018
Correlated	0.0101	0.0026	0.0010	0.0083	0.0060	0.010	0.0062	0.0013
Total Systematic	0.0116	0.0082	0.0059	0.0097	0.0088	0.016	0.0120	0.0022
$a(R_b)$		-0.0050						-0.1170
R_b^{used}		0.2159						0.2166
$a(\text{BR}(c \to \ell))$			-0.1646					
$\text{BR}(c \to \ell)^{\text{used}}$			9.80					

Table 21: The measurements of R_c^0. "c-count" denotes the determination of R_c^0 from the sum of production rates of weakly decaying charmed hadrons. "D meson" denotes any single/double tag analysis using exclusive and/or inclusive D meson reconstruction.

	ALEPH				DELPHI			L3	OPAL		
	90-95 lepton [38]	90-95 lepton [38]	90-95 lepton [38]	91-95† jet charge [42]	93-95† lepton [39]	92-95 D-meson [48]	92-95 jet charge [43]	90-95 lepton [40]	91-95 jet charge [46]	90-95† lepton [41]	90-95 D-meson [49]
$\sqrt{s}$ (GeV)	88.380	89.380	90.210	89.420	89.433	89.434	89.550	89.500	89.440	89.490	89.490
$A_{\rm FB}^{\rm bb}(-2)$	-3.53	5.47	9.11	4.66	5.90	5.65	6.80	6.14	4.10	3.56	-9.30
$A_{\rm FB}^{\rm bb}(-2)$Corrected		5.87		4.97	6.18	5.93	6.80	6.26	4.36	3.70	-9.16
Statistical		1.90		1.26	2.20	7.59	1.80	2.93	2.10	1.73	10.80
Uncorrelated		0.39		0.06	0.08	0.91	0.12	0.37	0.25	0.16	2.51
Correlated		0.70		0.01	0.08	0.08	0.01	0.19	0.02	0.04	1.41
Total Systematic		0.80		0.06	0.12	0.91	0.13	0.41	0.25	0.16	2.88
$a(R_{\rm b})$		-0.3069		-9.5	-1.1543		-0.1962	-1.4467	-0.7300	-0.1000	
$R_{\rm b}^{\rm used}$		0.2192		0.2150	0.2164		0.2158	0.2170	0.2150	0.2155	
$a(R_{\rm c})$		0.0362		0.3100	1.0444		0.3200	0.3612	0.0700	0.1000	
$R_{\rm c}^{\rm used}$		0.1710		0.1725	0.1671		0.1720	0.1734	0.1730	0.1720	
$a(A_{\rm FB}^{\rm cc}(-2))$		-0.2244		-0.2644				-0.1000	-0.3156		
$A_{\rm FB}^{\rm cc}(-2)^{\rm used}$		-2.34		-2.57				-2.50	-2.81		
$a({\rm BR(b}\to\ell))$		-0.2486			-1.0154			-1.0290		0.3406	
${\rm BR(b}\to\ell)^{\rm used}$		11.34			10.56			10.50		10.90	
$a({\rm BR(b}\to{\rm c}\to\bar{\ell}))$		-0.1074			-0.1424			-0.1440		-0.5298	
${\rm BR(b}\to{\rm c}\to\bar{\ell})^{\rm used}$		7.86			8.07			8.00		8.30	
$a({\rm BR(c}\to\ell))$		-0.0474			0.7224			0.5096		0.1960	
${\rm BR(c}\to\ell)^{\rm used}$		9.80			9.90			9.80		9.80	
$a(\overline{\chi})$		5.259			1.3054						
$\overline{\chi}^{\rm used}$		0.12460			0.11770						
$a(f({\rm D}^+))$						0.5083	0.0949				
$f({\rm D}^+)^{\rm used}$						0.2210	0.2330				
$a(f({\rm D_s}))$						0.1742	0.0035				
$f({\rm D_s})^{\rm used}$						0.1120	0.1020				
$a(f(\Lambda_{\rm c}))$						-0.0191	-0.0225				
$f(\Lambda_{\rm c})^{\rm used}$						0.0840	0.0630				

Table 22: The measurements of $A_{\rm FB}^{\rm b\bar{b}}(-2)$. All numbers are given in %.

	ALEPH	DELPHI		OPAL	
	91-95 D-meson [47]	93-95† lepton [39]	92-95 D-meson [48]	90-95† lepton [41]	90-95 D-meson [49]
$\sqrt{s}$ (GeV)	89.370	89.433	89.434	89.490	89.490
$A_{\rm FB}^{\rm cc}(-2)$	-1.10	1.11	-5.04	-6.92	3.90
$A_{\rm FB}^{\rm cc}(-2)$Corrected	-0.02	1.81	-4.35	-6.56	4.26
Statistical	4.30	3.60	3.69	2.44	5.10
Uncorrelated	1.00	0.53	0.40	0.38	0.80
Correlated	0.09	0.16	0.09	0.23	0.30
Total Systematic	1.00	0.55	0.41	0.44	0.86
$a(R_{\rm b})$		-0.2886		-3.4000	
$R_{\rm b}^{\rm used}$		0.2164		0.2155	
$a(R_{\rm c})$		1.0096	3.2000		
$R_{\rm c}^{\rm used}$		0.1671	0.1720		
$a(A_{\rm FB}^{\rm bb}(-2))$	-1.3365				
$A_{\rm FB}^{\rm bb}(-2)^{\rm used}$	6.13				
$a({\rm BR(b}\to\ell))$		-1.0966		-1.7031	
${\rm BR(b}\to\ell)^{\rm used}$		10.56		10.90	
$a({\rm BR(b}\to{\rm c}\to\bar{\ell}))$		1.1156		-1.4128	
${\rm BR(b}\to{\rm c}\to\bar{\ell})^{\rm used}$		8.07		8.30	
$a({\rm BR(c}\to\ell))$		1.0703		3.3320	
${\rm BR(c}\to\ell)^{\rm used}$		9.90		9.80	
$a(\overline{\chi})$		-0.0856			
$\overline{\chi}^{\rm used}$		0.11770			
$a(f({\rm D}^+))$			-0.3868		
$f({\rm D}^+)^{\rm used}$			0.2210		
$a(f({\rm D_s}))$			-0.1742		
$f({\rm D_s})^{\rm used}$			0.1120		
$a(f(\Lambda_{\rm c}))$			-0.0878		
$f(\Lambda_{\rm c})^{\rm used}$			0.0840		

Table 23: The measurements of $A_{\rm FB}^{\rm c\bar{c}}(-2)$. All numbers are given in %.

	ALEPH		DELPHI					L3		OPAL		
	91-95† lepton [38]	91-95† jet charge [42]	91-92 lepton [39]	93-95† lepton [39]	92-95 D-meson [48]	92-95 jet charge [43]	92-95† multi [44]	91-95 jet charge [45]	90-95 lepton [40]	91-95 jet charge [46]	90-95† lepton [41]	90-95 D-meson [49]
$\sqrt{s}$ (GeV)	91.210	91.230	91.270	91.223	91.235	91.260	91.260	91.240	91.260	91.210	91.240	91.240
$A_{\rm FB}^{\rm bb}$(pk)	9.71	9.90	10.89	9.86	7.59	9.83	9.31	9.31	9.85	10.06	9.14	8.90
$A_{\rm FB}^{\rm bb}$(pk)Corrected	9.81	9.96	10.87	9.93	7.63	9.83	9.31	9.35	9.85	10.15	9.18	8.94
Statistical	0.40	0.27	1.30	0.64	1.97	0.47	0.34	1.01	0.67	0.52	0.44	2.70
Uncorrelated	0.16	0.14	0.33	0.15	0.76	0.13	0.15	0.51	0.27	0.41	0.14	2.15
Correlated	0.12	0.01	0.27	0.14	0.10	0.04	0.02	0.21	0.14	0.20	0.15	0.45
Total Systematic	0.20	0.14	0.43	0.20	0.77	0.14	0.15	0.55	0.31	0.46	0.20	2.20
$a(R_{\rm b})$	-0.9545	-9.5	-2.8933	-2.0201		-0.1962	-0.2824	-9.1622	-2.1700	-7.6300	-0.7000	
$R_{\rm b}^{\rm used}$	0.2172	0.2158	0.2170	0.2164		0.2158	0.2165	0.2170	0.2170	0.2150	0.2155	
$a(R_{\rm c})$	0.6450	0.3100	1.0993	1.1488		0.8400	0.1558	1.0831	1.3005	0.4600	0.6000	
$R_{\rm c}^{\rm used}$	0.1720	0.1715	0.1710	0.1671		0.1720	0.1709	0.1733	0.1734	0.1730	0.1720	
$a(A_{\rm FB}^{\rm cc}({\rm pk}))$		0.6849					0.4173	1.1603	0.9262	0.6870		
$A_{\rm FB}^{\rm cc}({\rm pk})^{\rm used}$		6.66					6.89	6.91	7.41	6.19		
$a({\rm BR}({\rm b}\to\ell))$	-1.8480		-3.8824	-2.0308					-2.0160		-0.3406	
${\rm BR}({\rm b}\to\ell)^{\rm used}$	10.78		11.00	10.56					10.50		10.90	
$a({\rm BR}({\rm b}\to{\rm c}\to\bar{\ell}))$	0.4233		0.4740	-0.3798					-0.1280		-0.3532	
${\rm BR}({\rm b}\to{\rm c}\to\bar{\ell})^{\rm used}$	8.14		7.90	8.07					8.00		8.30	
$a({\rm BR}({\rm c}\to\ell))$	0.5096		0.7840	1.0703					1.5288		0.5880	
${\rm BR}({\rm c}\to\ell)^{\rm used}$	9.80		9.80	9.90					9.80		9.80	
$a(\overline{\chi})$	2.9904		3.4467	1.6692								
$\overline{\chi}^{\rm used}$	0.12460		0.12100	0.11770								
$a(f({\rm D}^+))$					0.0442	0.2761	0.4539					
$f({\rm D}^+)^{\rm used}$					0.2210	0.2330	0.2330					
$a(f({\rm D_s}))$					-0.0788	0.0106	0.1432					
$f({\rm D_s})^{\rm used}$					0.1120	0.1020	0.1020					
$a(f(\Lambda_{\rm c}))$					-0.0115	-0.0495	-0.0468					
$f(\Lambda_{\rm c})^{\rm used}$					0.0840	0.0630	0.0930					

Table 24: The measurements of $A_{\rm FB}^{\rm b\bar{b}}$(pk). All numbers are given in %.

	ALEPH			DELPHI			L3	OPAL		
	91-95† lepton [38]	91-95 D-meson [47]	91-92 lepton [39]	93-95† lepton [39]	92-95 D-meson [48]	92-95† lepton [39]	90-95 lepton [40]	90-95† lepton [41]	90-95 D-meson [49]
$\sqrt{s}$ (GeV)	91.210	91.220	91.270	91.223	91.235	91.223	91.240	91.240	91.240
$A_{\rm FB}^{\rm cc}$(pk)	5.69	6.20	8.05	6.28	6.58	6.28	7.94	5.97	6.60
$A_{\rm FB}^{\rm cc}$(pk)Corrected	5.94	6.39	8.00	6.46	6.70	6.46	8.04	6.07	6.70
Statistical	0.53	0.90	2.26	1.00	0.97	1.00	3.70	0.59	1.20
Uncorrelated	0.24	0.23	1.25	0.53	0.25	0.53	2.40	0.37	0.49
Correlated	0.36	0.17	0.49	0.27	0.04	0.27	0.49	0.32	0.24
Total Systematic	0.44	0.28	1.35	0.60	0.25	0.60	2.45	0.49	0.54
$a(R_{\rm b})$	1.4318		2.8933	-2.3087		-2.3087	4.3200	4.1000	
$R_{\rm b}^{\rm used}$	0.2172		0.2170	0.2164		0.2164	0.2160	0.2155	
$a(R_{\rm c})$	-2.9383		-6.4736	5.4307		5.4307	-6.7600	-3.8000	
$R_{\rm c}^{\rm used}$	0.1720		0.1710	0.1671		0.1671	0.1690	0.1720	
$a(A_{\rm FB}^{\rm bb}({\rm pk}))$		-2.1333					6.4274		
$A_{\rm FB}^{\rm bb}({\rm pk})^{\rm used}$		9.79					8.84		
$a({\rm BR}({\rm b}\to\ell))$	1.8993		4.8529	-2.7618			3.5007	5.1094	
${\rm BR}({\rm b}\to\ell)^{\rm used}$	10.78		11.00	10.56			10.50	10.90	
$a({\rm BR}({\rm b}\to{\rm c}\to\bar{\ell}))$	-1.0745		-3.9500	2.2786			-3.2917	-1.7660	
${\rm BR}({\rm b}\to{\rm c}\to\bar{\ell})^{\rm used}$	8.14		7.90	8.07			7.90	8.30	
$a({\rm BR}({\rm c}\to\ell))$	-3.2732		-7.2520	4.8965			-6.5327	-3.9200	
${\rm BR}({\rm c}\to\ell)^{\rm used}$	9.80		9.80	9.90			9.80	9.80	
$a(\overline{\chi})$	0.0453			0.3852					
$\overline{\chi}^{\rm used}$	0.12460			0.11770					
$a(f({\rm D}^+))$					-0.0221				
$f({\rm D}^+)^{\rm used}$					0.2210				
$a(f({\rm D_s}))$					0.0788				
$f({\rm D_s})^{\rm used}$					0.1120				
$a(f(\Lambda_{\rm c}))$					0.0115				
$f(\Lambda_{\rm c})^{\rm used}$					0.0840				

Table 25: The measurements of $A_{\rm FB}^{\rm c\bar{c}}$(pk). All numbers are given in %.

	ALEPH				DELPHI			L3	OPAL		
	90-95 lepton [38]	90-95 lepton [38]	90-95 lepton [38]	91-95† jet charge [42]	93-95† lepton [39]	92-95 D-meson [48]	92-95 jet charge [43]	90-95 lepton [40]	91-95 jet charge [46]	90-95† lepton [41]	90-95 D-meson [49]
$\sqrt{s}$ (GeV)	92.050	92.940	93.900	92.950	92.990	92.990	92.940	93.100	92.910	92.950	92.950
$A_{\rm FB}^{\rm b\bar{b}}(+2)$	3.93	10.60	9.03	11.82	10.10	8.78	12.30	13.78	14.60	10.75	-3.40
$A_{\rm FB}^{\rm b\bar{b}}(+2)$Corrected		10.03		11.81	10.05	8.73	12.30	13.62	14.63	10.74	-3.41
Statistical		1.51		0.99	1.80	6.37	1.60	2.40	1.70	1.43	9.00
Uncorrelated		0.14		0.16	0.14	0.97	0.25	0.34	0.64	0.25	2.03
Correlated		0.24		0.01	0.16	0.13	0.05	0.20	0.34	0.28	1.74
Total Systematic		0.28		0.16	0.21	0.98	0.26	0.40	0.73	0.37	2.68
$a(R_{\rm b})$		-1.964		-9.5	-2.8859		-0.1962	-3.3756	-12.9000	-0.8000	
$R_{\rm b}^{\rm used}$		0.2192		0.2156	0.2164		0.2158	0.2170	0.2150	0.2155	
$a(R_{\rm c})$		1.575		0.3100	1.3577		1.2000	1.9869	0.6900	0.8000	
$R_{\rm c}^{\rm used}$		0.1710		0.1719	0.1671		0.1720	0.1734	0.1730	0.1720	
$a(A_{\rm FB}^{\rm c\bar{c}}(+2))$		1.081		1.2793				0.5206	1.3287		
$A_{\rm FB}^{\rm c\bar{c}}(+2)^{\rm used}$		12.51		12.42				12.39	12.08		
$a({\rm BR}({\rm b}\to\ell))$		-1.762			-2.3557			-2.0790		-1.3625	
${\rm BR}({\rm b}\to\ell)^{\rm used}$		11.34			10.56			10.50		10.90	
$a({\rm BR}({\rm b}\to{\rm c}\to\bar{\ell}))$		-0.2478			-0.7595			-1.1200		0.7064	
${\rm BR}({\rm b}\to{\rm c}\to\bar{\ell})^{\rm used}$		7.86			8.07			8.00		8.30	
$a({\rm BR}({\rm c}\to\ell))$		1.524			1.0703			1.9796		0.7840	
${\rm BR}({\rm c}\to\ell)^{\rm used}$		9.80			9.90			9.80		9.80	
$a(\overline{\chi})$		6.584			1.6050						
$\overline{\chi}^{\rm used}$		0.12460			0.11770						
$a(f({\rm D}^+))$						0.3978	0.4229				
$f({\rm D}^+)^{\rm used}$						0.2210	0.2330				
$a(f({\rm D_s}))$						-0.0788	0.0211				
$f({\rm D_s})^{\rm used}$						0.1120	0.1020				
$a(f(\Lambda_{\rm c}))$						0.0573	-0.0855				
$f(\Lambda_{\rm c})^{\rm used}$						0.0840	0.0630				

Table 26: The measurements of $A_{\rm FB}^{\rm b\bar{b}}(+2)$. All numbers are given in %.

	ALEPH	DELPHI		OPAL	
	91-95 D-meson [47]	93-95† lepton [39]	92-95 D-meson [48]	90-95† lepton [41]	90-95 D-meson [49]
$\sqrt{s}$ (GeV)	92.960	92.990	92.990	92.950	92.950
$A_{\rm FB}^{\rm c\bar{c}}(+2)$	10.94	10.50	11.78	15.65	16.70
$A_{\rm FB}^{\rm c\bar{c}}(+2)$Corrected	10.89	10.37	11.65	15.62	16.67
Statistical	3.30	2.90	3.20	2.02	4.10
Uncorrelated	0.79	0.41	0.52	0.57	0.92
Correlated	0.18	0.29	0.07	0.62	0.51
Total Systematic	0.81	0.50	0.52	0.84	1.05
$a(R_{\rm b})$		-4.0402		9.6000	
$R_{\rm b}^{\rm used}$		0.2164		0.2155	
$a(R_{\rm c})$		7.5891		-8.9000	
$R_{\rm c}^{\rm used}$		0.1671		0.1720	
$a(A_{\rm FB}^{\rm b\bar{b}}(+2))$	-2.6333				
$A_{\rm FB}^{\rm b\bar{b}}(+2)^{\rm used}$	12.08				
$a({\rm BR}({\rm b}\to\ell))$		-3.2492		9.5375	
${\rm BR}({\rm b}\to\ell)^{\rm used}$		10.56		10.90	
$a({\rm BR}({\rm b}\to{\rm c}\to\bar{\ell}))$		1.5191		-1.5894	
${\rm BR}({\rm b}\to{\rm c}\to\bar{\ell})^{\rm used}$		8.07		8.30	
$a({\rm BR}({\rm c}\to\ell))$		8.1341		-9.2120	
${\rm BR}({\rm c}\to\ell)^{\rm used}$		9.90		9.80	
$a(\overline{\chi})$		-0.2140			
$\overline{\chi}^{\rm used}$		0.11770			
$a(f({\rm D}^+))$			-0.2984		
$f({\rm D}^+)^{\rm used}$			0.2210		
$a(f({\rm D_s}))$			0.0539		
$f({\rm D_s})^{\rm used}$			0.1120		
$a(f(\Lambda_{\rm c}))$			0.0764		
$f(\Lambda_{\rm c})^{\rm used}$			0.0840		

Table 27: The measurements of $A_{\rm FB}^{\rm c\bar{c}}(+2)$. All numbers are given in %.

	SLD			
	93-98† lepton [50]	93-98† jet charge [53]	94-95† $K^{\pm}$ [54]	96-98† multi [55]
$\sqrt{s}$ (GeV)	91.280	91.280	91.280	91.280
$\mathcal{A}_{\rm b}$	0.922	0.907	0.855	0.913
Statistical	0.029	0.020	0.088	0.019
Uncorrelated	0.019	0.023	0.102	0.018
Correlated	0.008	0.001	0.006	0.001
Total Systematic	0.021	0.024	0.102	0.018
$a(R_{\rm b})$	-0.0542		-0.0139	-0.4586
$R_{\rm b}^{\rm used}$	0.2168		0.2180	0.2158
$a(R_{\rm c})$	0.0424		0.0060	0.0215
$R_{\rm c}^{\rm used}$	0.1697		0.1710	0.1722
$a(\mathcal{A}_{\rm c})$	0.0449	0.0211	-0.0112	0.0076
$\mathcal{A}_{\rm c}{}^{\rm used}$	0.667	0.670	0.666	0.667
$a({\rm BR}({\rm b}\to\ell))$	-0.2160			
${\rm BR}({\rm b}\to\ell)^{\rm used}$	10.80			
$a({\rm BR}({\rm b}\to{\rm c}\to\bar{\ell}))$	0.0888			
${\rm BR}({\rm b}\to{\rm c}\to\bar{\ell})^{\rm used}$	8.05			
$a({\rm BR}({\rm c}\to\ell))$	0.0479			
${\rm BR}({\rm c}\to\ell)^{\rm used}$	9.83			
$a(\overline{\chi})$	0.3052			
$\overline{\chi}^{\rm used}$	0.11990			

Table 28: The measurements of $\mathcal{A}_{\rm b}$.

	SLD		
	93-98† lepton [51]	93-98† D-meson [52]	96-98† K+vertex [56]
$\sqrt{s}$ (GeV)	91.280	91.280	91.280
$\mathcal{A}_{\rm c}$	0.567	0.688	0.674
Statistical	0.051	0.035	0.029
Uncorrelated	0.056	0.020	0.025
Correlated	0.018	0.003	0.002
Total Systematic	0.059	0.021	0.025
$a(R_{\rm b})$	0.2173		0.1888
$R_{\rm b}^{\rm used}$	0.2173		0.2158
$a(R_{\rm c})$	-0.4089		-0.0430
$R_{\rm c}^{\rm used}$	0.1730		0.1722
$a(\mathcal{A}_{\rm b})$	0.2151	-0.0673	-0.0160
$\mathcal{A}_{\rm b}{}^{\rm used}$	0.935	0.935	0.935
$a({\rm BR}({\rm b}\to\ell))$	0.2328		
${\rm BR}({\rm b}\to\ell)^{\rm used}$	11.06		
$a({\rm BR}({\rm b}\to{\rm c}\to\bar{\ell}))$	-0.1178		
${\rm BR}({\rm b}\to{\rm c}\to\bar{\ell})^{\rm used}$	8.02		
$a({\rm BR}({\rm c}\to\ell))$	-0.4077		
${\rm BR}({\rm c}\to\ell)^{\rm used}$	9.80		
$a(\overline{\chi})$	0.1138		
$\overline{\chi}^{\rm used}$	0.12170		

Table 29: The measurements of $\mathcal{A}_{\rm c}$.

	ALEPH	DELPHI	L3		OPAL
	91-95† multi [57]	94-95† multi [58]	92 lepton [59]	94-95† multi [27]	92-95 multi [60]
$BR(b \to \ell)$	10.55	10.65	10.68	10.21	10.83
Statistical	0.09	0.07	0.11	0.13	0.10
Uncorrelated	0.17	0.23	0.36	0.20	0.20
Correlated	0.22	0.42	0.22	0.31	0.21
Total Systematic	0.27	0.48	0.42	0.36	0.29
$a(R_b)$			-9.2571		-0.1808
R_b^{used}			0.2160		0.2169
$a(R_c)$				1.4450	0.4867
R_c^{used}				0.1734	0.1770
$a(BR(b \to c \to \ell))$			-1.1700	0.1618	
$BR(b \to c \to \bar{\ell})^{used}$			9.00	8.09	
$a(BR(c \to \ell))$	-0.3078	-0.1960	-2.5480	0.9212	
$BR(c \to \ell)^{used}$	9.85	9.80	9.80	9.80	
$a(\overline{\chi})$	0.7683				
$\overline{\chi}^{used}$	0.1178				
$a(f(D^+))$				0.5523	0.1445
$f(D^+)^{used}$				0.2330	0.2380
$a(f(D_s))$				0.0213	0.0055
$f(D_s)^{used}$				0.1030	0.1020
$a(f(\Lambda_c))$				-0.0427	-0.0157
$f(\Lambda_c)^{used}$				0.0630	0.0650

Table 30: The measurements of $BR(b \to \ell)$. All numbers are given in %.

	ALEPH	DELPHI	OPAL
	91-95† multi [57]	94-95† multi [58]	92-95 multi [60]
$BR(b \to c \to \bar{\ell})$	8.04	7.88	8.40
Statistical	0.14	0.13	0.16
Uncorrelated	0.20	0.26	0.19
Correlated	0.14	0.36	0.34
Total Systematic	0.25	0.45	0.39
$a(R_b)$			-0.1808
R_b^{used}			0.2169
$a(R_c)$	0.8916		0.3761
R_c^{used}	0.1694		0.1770
$a(BR(c \to \ell))$	0.3078	-0.1960	
$BR(c \to \ell)^{used}$	9.85	9.80	
$a(\overline{\chi})$	-1.2804		
$\overline{\chi}^{used}$	0.11780		
$a(f(D^+))$			0.1190
$f(D^+)^{used}$			0.2380
$a(f(D_s))$			0.0028
$f(D_s)^{used}$			0.1020
$a(f(\Lambda_c))$			-0.0110
$f(\Lambda_c)^{used}$			0.0660

Table 31: The measurements of $BR(b \to c \to \bar{\ell})$. All numbers are given in %.

	DELPHI	OPAL
	92-95 D+lepton [31]	90-95 D+lepton [61]
$BR(c \to \ell)$	9.59	9.60
Statistical	0.42	0.60
Uncorrelated	0.24	0.49
Correlated	0.14	0.43
Total Systematic	0.27	0.65
$a(BR(b \to \ell))$	-0.5600	-1.4335
$BR(b \to \ell)^{used}$	11.20	10.99
$a(BR(b \to c \to \bar{\ell}))$	-0.4100	-0.7800
$BR(b \to c \to \bar{\ell})^{used}$	8.20	7.80

Table 32: The measurements of $BR(c \to \ell)$. All numbers are given in %.

	ALEPH	DELPHI	L3	OPAL
	90-95 multi [38]	94-95† multi [58]	90-95 lepton [40]	90-95† lepton [41]
$\overline{\chi}$	0.12461	0.12700	0.11920	0.11390
Statistical	0.00515	0.01300	0.00680	0.00540
Uncorrelated	0.00252	0.00566	0.00214	0.00306
Correlated	0.00397	0.00554	0.00252	0.00324
Total Systematic	0.00470	0.00792	0.00330	0.00446
$a(R_{\mathrm{b}})$	0.0341		0.0000	
$R_{\mathrm{b}}^{\mathrm{used}}$	0.2192		0.2170	
$a(R_{\mathrm{c}})$	0.0009		0.0004	
$R_{\mathrm{c}}^{\mathrm{used}}$	0.1710		0.1734	
$a(\mathrm{BR}(\mathrm{b} \to \ell))$	0.0524		0.0550	0.0170
$\mathrm{BR}(\mathrm{b} \to \ell)^{\mathrm{used}}$	11.34		10.50	10.90
$a(\mathrm{BR}(\mathrm{b} \to \mathrm{c} \to \bar{\ell}))$	-0.0440		-0.0466	-0.0318
$\mathrm{BR}(\mathrm{b} \to \mathrm{c} \to \bar{\ell})^{\mathrm{used}}$	7.86		8.00	8.30
$a(\mathrm{BR}(\mathrm{c} \to \ell))$	0.0035	-0.0020	0.0006	0.0039
$\mathrm{BR}(\mathrm{c} \to \ell)^{\mathrm{used}}$	9.80	9.80	9.80	9.80

Table 33: The measurements of $\overline{\chi}$.

	DELPHI	OPAL
	92-95 D-meson [31]	90-95 D-meson [33]
$\mathrm{P}(\mathrm{c} \to \mathrm{D}^{*+}) \times \mathrm{BR}(\mathrm{D}^{*+} \to \pi^+\mathrm{D}^0)$	0.1740	0.1513
Statistical	0.0100	0.0096
Uncorrelated	0.0040	0.0088
Correlated	0.0007	0.0011
Total Systematic	0.0041	0.0089
$a(R_{\mathrm{b}})$	0.0293	
$R_{\mathrm{b}}^{\mathrm{used}}$	0.2166	
$a(R_{\mathrm{c}})$	-0.0158	
$R_{\mathrm{c}}^{\mathrm{used}}$	0.1735	

Table 34: The measurements of $\mathrm{P}(\mathrm{c} \to \mathrm{D}^{*+}) \times \mathrm{BR}(\mathrm{D}^{*+} \to \pi^+\mathrm{D}^0)$.

	ALEPH	DELPHI	OPAL
	91-95 D meson [34]	92-95 D meson [32]	91-94 D meson [35]
$\mathrm{R_c f_{D^+}}$	0.0406	0.0384	0.0390
Statistical	0.0013	0.0013	0.0050
Uncorrelated	0.0014	0.0015	0.0042
Correlated	0.0032	0.0025	0.0031
Total Systematic	0.0035	0.0030	0.0052
$a(f(\mathrm{D}^+))$		0.0008	
$f(\mathrm{D}^+)^{\mathrm{used}}$		0.2210	
$a(f(\mathrm{D_s}))$		-0.0002	
$f(\mathrm{D_s})^{\mathrm{used}}$		0.1120	
$a(f(\Lambda_{\mathrm{c}}))$		0.0000	
$f(\Lambda_{\mathrm{c}})^{\mathrm{used}}$		0.0840	

Table 35: The measurements of $\mathrm{R_c f_{D^+}}$.

	ALEPH	DELPHI	OPAL
	91-95 D meson [34]	92-95 D meson [32]	91-94 D meson [35]
$\mathrm{R_c f_{D_s}}$	0.0207	0.0213	0.0160
Statistical	0.0033	0.0017	0.0042
Uncorrelated	0.0011	0.0010	0.0016
Correlated	0.0053	0.0054	0.0043
Total Systematic	0.0054	0.0055	0.0046
$a(f(\mathrm{D}^+))$		0.0007	
$f(\mathrm{D}^+)^{\mathrm{used}}$		0.2210	
$a(f(\mathrm{D_s}))$		-0.0009	
$f(\mathrm{D_s})^{\mathrm{used}}$		0.1120	
$a(f(\Lambda_{\mathrm{c}}))$		-0.0001	
$f(\Lambda_{\mathrm{c}})^{\mathrm{used}}$		0.0840	

Table 36: The measurements of $\mathrm{R_c f_{D_s}}$.

	ALEPH	DELPHI	OPAL
	91-95 D meson [34]	92-95 D meson [32]	91-94 D meson [35]
$R_c f_{\Lambda_c}$	0.0157	0.0169	0.0091
Statistical	0.0016	0.0035	0.0050
Uncorrelated	0.0005	0.0016	0.0015
Correlated	0.0044	0.0045	0.0035
Total Systematic	0.0045	0.0048	0.0038
$a(f(D^+))$		0.0002	
$f(D^+)^{used}$		0.2210	
$a(f(D_s))$		-0.0001	
$f(D_s)^{used}$		0.1120	
$a(f(\Lambda_c))$		-0.0002	
$f(\Lambda_c)^{used}$		0.0840	

Table 37: The measurements of $R_c f_{\Lambda_c}$.

	ALEPH	DELPHI	OPAL
	91-95 D meson [34]	92-95 D meson [32]	91-94 D meson [35]
$R_c f_{D^0}$	0.0964	0.0926	0.0997
Statistical	0.0029	0.0026	0.0070
Uncorrelated	0.0040	0.0038	0.0057
Correlated	0.0045	0.0023	0.0041
Total Systematic	0.0060	0.0044	0.0070
$a(f(D^+))$		0.0020	
$f(D^+)^{used}$		0.2210	
$a(f(D_s))$		-0.0004	
$f(D_s)^{used}$		0.1120	
$a(f(\Lambda_c))$		-0.0004	
$f(\Lambda_c)^{used}$		0.0840	

Table 38: The measurements of $R_c f_{D^0}$.

	DELPHI	OPAL
	92-95 D meson [32]	90-95 D-meson [33]
$R_c P(c \to D^{*+}) \times BR(D^{*+} \to \pi^+ D^0)$	0.0282	0.0266
Statistical	0.0007	0.0005
Uncorrelated	0.0010	0.0010
Correlated	0.0007	0.0009
Total Systematic	0.0012	0.0014
$a(f(D^+))$	0.0006	
$f(D^+)^{used}$	0.2210	
$a(f(D_s))$	-0.0001	
$f(D_s)^{used}$	0.1120	
$a(f(\Lambda_c))$	-0.0004	
$f(\Lambda_c)^{used}$	0.0840	

Table 39: The measurements of $R_c P(c \to D^{*+}) \times BR(D^{*+} \to \pi^+ D^0)$.

References

[1] The LEP Collaborations ALEPH, DELPHI, L3, OPAL and the LEP Electroweak Working Group, and the SLD Heavy Flavour and Electroweak Groups, *A Combination of Preliminary Electroweak Measurements and Constraints on the Standard Model*, CERN–EP-2001-21, hep-ex/0103048.

[2] The LEP Collaborations ALEPH, DELPHI, L3 and OPAL and the LEP Electroweak working group, *Combination procedure for the precise determination of Z boson parameters from results of the LEP experiments*, CERN–EP-2000-153, hep-ex/0101027.

[3] The LEP Experiments: ALEPH, DELPHI, L3 and OPAL, Nucl. Inst. Meth. **A378** (1996) 101.

[4] ALEPH Collaboration, D. Decamp *et al.*, Z. Phys. **C48** (1990) 365;
ALEPH Collaboration, D. Decamp *et al.*, Z. Phys. **C53** (1992) 1;
ALEPH Collaboration, D. Buskulic *et al.*, Z. Phys. **C60** (1993) 71;
ALEPH Collaboration, D. Buskulic *et al.*, Z. Phys. **C62** (1994) 539;
ALEPH Collaboration, R. Barate *et al.*, Eur. Phys. J. **C 14** (2000) 1.

[5] DELPHI Collaboration, P. Aarnio *et al.*, Nucl. Phys. **B367** (1991) 511;
DELPHI Collaboration, P. Abreu *et al.*, Nucl. Phys. **B417** (1994) 3;
DELPHI Collaboration, P. Abreu *et al.*, Nucl. Phys. **B418** (1994) 403;
DELPHI Collaboration, P. Abreu *et al.*, Eur. Phys. J. **C 16** (2000) 371.

[6] L3 Collaboration, B. Adeva *et al.*, Z. Phys. **C51** (1991) 179;
L3 Collaboration, O. Adriani *et al.*, Phys. Rep. **236** (1993) 1;
L3 Collaboration, M. Acciarri *et al.*, Z. Phys. **C62** (1994) 551;
L3 Collaboration, M. Acciarri *et al.*, Eur. Phys. J. **C16** (2000) 1-40.

[7] OPAL Collaboration, G. Alexander *et al.*, Z. Phys. **C52** (1991) 175;
OPAL Collaboration, P.D. Acton *et al.*, Z. Phys. **C58** (1993) 219;
OPAL Collaboration, R. Akers *et al.*, Z. Phys. **C61** (1994) 19;
OPAL Collaboration, G. Abbiendi *et al.*, Eur. Phys. J. **C14** (2000) 373;
OPAL Collaboration, G. Abbiendi *et al.*, Eur. Phys. J. **C19** (2001) 587.

[8] F.A. Berends et al., in *Z Physics at LEP 1, Vol. 1*, ed. G. Altarelli, R. Kleiss and C. Verzegnassi, (CERN Report: CERN 89-08, 1989), p. 89.
M. Böhm et al., in *Z Physics at LEP 1, Vol. 1*, ed. G. Altarelli, R. Kleiss and C. Verzegnassi, (CERN Report: CERN 89-08, 1989), p. 203.

[9] See, for example, M. Consoli *et al.*, in "Z Physics at LEP 1", CERN Report CERN 89-08 (1989), eds G. Altarelli, R. Kleiss and C. Verzegnassi, Vol. 1, p. 7.

[10] S. Jadach, *et al.*, Phys. Lett. **B257** (1991) 173.

[11] M. Skrzypek, Acta Phys. Pol. **B23** (1992) 135.

[12] G. Montagna, *et al.*, Phys. Lett. **B406** (1997) 243.

[13] G. Montagna *et al.*, Nucl. Phys. **B547** (1999) 39;
G. Montagna *et al.*, Phys. Rev. Lett. **459** (1999) 649.

[14] B.F.L Ward *et al.*, Phys. Lett. **B450** (1999) 262.

[15] D. Bardin, M. Grünewald and G. Passarino, *Precision Calculation Project Report*, hep-ph/9902452.

[16] ALEPH Collaboration, D. Buskulic *et al.*, Zeit. Phys. **C69** (1996) 183;
ALEPH Collaboration, *Measurement of the tau polarisation by ALEPH with the full LEP I data sample*, ALEPH 96-067 CONF 98-037, contributed paper to ICHEP 98 Vancouver **ICHEP'98 #939**.

[17] DELPHI Collaboration, P. Abreu *et al.*, Eur. Phys. J. **C14** (2000) 585.

[18] L3 Collaboration, M. Acciarri *et al.*, Phys. Lett. **B429** (1998) 387.

[19] OPAL Collaboration, G. Abbiendi *et al.*, *Precision Neutral Current Asymmetry Parameter Measurements from the Tau Polarization at LEP*, CERN-EP-2001-023, Submitted to Eur. Phys. J. C.

[20] The LEP Collaborations ALEPH, DELPHI, L3, OPAL and the LEP Electroweak Working Group, *Combined Preliminary Data on* Z *Parameters from the LEP Experiments and Constraints on the Standard Model*, CERN–PPE/94-187.

[21] SLD Collaboration, K. Abe *et al.*, Phys. Rev. Lett. **84** (2000) 5945.

[22] SLD Collaboration, K. Abe *et al.*, SLAC-PUB-8618, (2000). Submitted to Phys.Rev.Lett.

[23] The LEP Heavy Flavour Group, *Input Parameters for the LEP/SLD Electroweak Heavy Flavour Results for Summer 1998 Conferences* , LEPHF/98-01,
http://www.cern.ch/LEPEWWG/heavy/lephf9801.ps.gz.

[24] The LEP Collaborations ALEPH, DELPHI, L3, OPAL and the LEP Electroweak Working Group, and the SLD Heavy Flavour and Electroweak Groups, *A Combination of Preliminary Electroweak Measurements and Constraints on the Standard Model*, CERN–EP-2000-16.

[25] ALEPH Collaboration, R. Barate *et al.*, Physics Letters **B 401** (1997) 150;
ALEPH Collaboration, R. Barate *et al.*, Physics Letters **B 401** (1997) 163.

[26] DELPHI Collaboration, P.Abreu *et al.*, Eur. Phys. J. **C10** (1999) 415.

[27] L3 Collaboration, M. Acciarri *et al.*, Eur. Phys. J. **C13** (2000) 47.

[28] OPAL Collaboration, G. Abbiendi *et al.*, Eur. Phys. J. **C8** (1999) 217.

[29] SLD Collaboration, *Improved measurement of* R_b, R_c *at SLD*, SLAC-PUB-8667, Contributed Paper to ICHEP2000 , **# 739**;
N. De Groot *Electroweak results from SLD*, talk prsented at XXXVIth Rencontres de Moriond, Electroweak Interactions and Unified Theories, Les Arcs, March 2001, hep-ex/0105058.

[30] ALEPH Collaboration, R. Barate *et al.*, Eur. Phys. J. **C4** (1998) 557.

[31] DELPHI Collaboration, P.Abreu *et al.*, Eur. Phys. J. **C12** (2000) 209.

[32] DELPHI Collaboration, P.Abreu *et al.*, Eur. Phys. J. **C12** (2000) 225.

[33] OPAL Collaboration, K. Ackerstaff *et al.*, Eur. Phys. J. **C1** (1998) 439.

[34] ALEPH Collaboration, R. Barate *et al.*, Eur. Phys. J. **C16** (2000) 597.

[35] OPAL Collaboration, G. Alexander *et al.*, Z. Phys. **C72** (1996) 1.

[36] D. Abbaneo *et al.*, Eur. Phys. J. **C4** (1998) 185.

[37] D. Bardin *et al.*, Z. Phys. **C44** (1989) 493; Comp. Phys. Comm. **59** (1990) 303; Nucl. Phys. **B351**(1991) 1; Phys. Lett. **B255** (1991) 290 and CERN-TH 6443/92 (May 1992); the most recent version of ZFITTER (6.21) is described in DESY 99-070, hep-ph/9908433 (Aug 1999) published in Comp. Phys. Comm. **133** (2001) 229.

[38] ALEPH Collaboration, D. Buskulic *et al.*, Phys. Lett. **B384** (1996)414;
ALEPH Collaboration, *Measurement of the b and c forward-backward asymmetries using leptons* ALEPH 99-076 CONF 99-048, contributed paper to EPS 99 Tampere **HEP'99 #6-65**.

[39] DELPHI Collaboration, P.Abreu *et al.*, Z. Phys **C65** (1995) 569;
DELPHI Collaboration, *Measurement of the Forward-Backward Asymmetries of* $e^+e^- \rightarrow Z \rightarrow b\bar{b}$ *and* $e^+e^- \rightarrow Z \rightarrow c\bar{c}$ *using prompt leptons* DELPHI 2000-101 CONF 400, contributed paper to ICHEP 2000 Osaka **ICHEP'00 #377** .
Delphi notes are available at http://wwwcn.cern.ch/~pubxx/www/delsec/delnote/.

[40] L3 Collaboration, O. Adriani *et al.*, Phys. Lett. **B292** (1992) 454;
L3 Collaboration, *L3 Results on* $A_{\rm FB}^{\rm b\bar{b}}$, $A_{\rm FB}^{\rm c\bar{c}}$ *and* χ *for the Glasgow Conference,* L3 Note 1624;
L3 Collaboration, M. Acciarri *et al.*, Phys. Lett. **B448** (1999) 152.

[41] OPAL Collaboration, G. Alexander *et al.*, Z. Phys. **C70** (1996) 357;
OPAL Collaboration, R. Akers *et al.*, *Updated Measurement of the Heavy Quark Forward-Backward Asymmetries and Average B Mixing Using Leptons in Multihadronic Events*, OPAL Physics Note PN226 contributed paper to ICHEP96, Warsaw, 25-31 July 1996 **PA05-007**
OPAL Collaboration, R. Akers *et al.*, *QCD corrections to the bottom and charm forward-backward asymmetries* OPAL Physics Note PN284.

[42] ALEPH Collaboration, *Measurement of* $A_F B^b$ *using Inclusive b-hadron Decays*, ALEPH 2001-026 CONF 2001-020.

[43] DELPHI Collaboration, P.Abreu *et al.*, Eur. Phys. J. **C9** (1999) 367.

[44] DELPHI Collaboration, *Determination of* $A_F B^b$ *using inclusive charge reconstruction and lifetime tagging at LEP 1*, DELPHI 2001-027 CONF 468.

[45] L3 Collaboration, M. Acciarri *et al.*, Phys. Lett. **B439** (1998) 225.

[46] OPAL Collaboration, K.Ackerstaff *et al.*, Z. Phys. **C75** (1997) 385.

[47] ALEPH Collaboration, R. Barate *et al.*, Phys. Lett. **B434** (1998) 415.

[48] DELPHI Collaboration, P.Abreu *et al.*, Eur. Phys. J. **C10** (1999) 219.

[49] OPAL Collaboration, G. Alexander *et al.*, Z. Phys. **C73** (1996) 379.

[50] SLD Collaboration, *Direct measurement of* $\mathcal{A}_b$ *at the* Z^0 *Pole using a lepton tag*, SLAC-PUB-8516, Contributed Paper to ICHEP2000 , **# 741**;
N. De Groot *Electroweak results from SLD*, talk prsented at XXXVIth Rencontres de Moriond, Electroweak Interactions and Unified Theories, Les Arcs, March 2001, hep-ex/0105058.

[51] SLD Collaboration, SLAC–PUB–7637, contributed paper to EPS-HEP-97, Jerusalem, **EPS-124**;
N. De Groot *Electroweak results from SLD*, talk prsented at XXXVIth Rencontres de Moriond, Electroweak Interactions and Unified Theories, Les Arcs, March 2001, hep-ex/0105058.

[52] SLD Collaboration, K. Abe, *et al.*, Phys Rev. **D63** 032005 (2001).

[53] SLD Collaboration, *Measurement of* $\mathcal{A}_b$ *at the Z resonance using a Jet-Charge Technique* SLAC–PUB–7886, contributed paper to ICHEP 98 Vancouver **ICHEP'98 #179** ;
N. De Groot *Electroweak results from SLD*, talk prsented at XXXVIth Rencontres de Moriond, Electroweak Interactions and Unified Theories, Les Arcs, March 2001, hep-ex/0105058.

[54] SLD Collaboration, K. Abe et al, Phys. Rev. Lett. **83**, 1902 (1999).

[55] SLD Collaboration, *Direct measurement of* $\mathcal{A}_b$ *using charged kaons at the SLD detector*, SLAC-PUB-8200, contributed paper to EPS 99 Tampere **HEP'99 #6_473** ;
SLD Collaboration, *Direct measurement of Ab using charged vertices*, SLAC-PUB-8542, Contributed Paper to ICHEP2000 , **# 743**;
N. De Groot *Electroweak results from SLD*, talk prsented at XXXVIth Rencontres de Moriond, Electroweak Interactions and Unified Theories, Les Arcs, March 2001, hep-ex/0105058.

[56] SLD Collaboration, *Direct measurement of* $\mathcal{A}_c$ *using inclusive charm tagging at the SLD detector*, SLAC-PUB-8199, contributed paper to EPS 99 Tampere **HEP'99 #6_474** ;
N. De Groot *Electroweak results from SLD*, talk prsented at XXXVIth Rencontres de Moriond, Electroweak Interactions and Unified Theories, Les Arcs, March 2001, hep-ex/0105058.

[57] ALEPH Collaboration. , *Inclusive semileptonic branching ratios of b hadrons produced in Z decays*, ALEPH 2000-069 CONF 2000-047, Contributed Paper to ICHEP2000 , **# 182**.

[58] DELPHI Collaboration, *Measurement of the semileptonic b branching ratios in Z decays* DELPHI 99-111 CONF 298, contributed paper to EPS 99 Tampere **HEP'99 #5_522** .

[59] L3 Collaboration, M. Acciarri *et al.*, Z Phys. **C71** 379 (1996).

[60] OPAL Collaboration, G. Abbiendi *et al.*, Eur. Phys. J. **C13** (2000) 225.

[61] OPAL Collaboration, G. Abbiendi *et al.*, Eur. Phys. J. **C8** (1999) 573.

[62] ALEPH Collaboration, D. Decamp *et al.*, Phys. Lett. **B259** (1991) 377.

[63] ALEPH Collaboration, ALEPH-Note 93-041 PHYSIC 93-032 (1993);
ALEPH Collaboration, ALEPH-Note 93-042 PHYSIC 93-033 (1993);
ALEPH Collaboration, ALEPH-Note 93-044 PHYSIC 93-035 (1993).

[64] ALEPH Collaboration, D. Buskulic *et al.*, Z. Phys. **C71** (1996) 357.

[65] DELPHI Collaboration, P. Abreu *et al.*, Phys. Lett. **B277** (1992) 371.

[66] DELPHI Collaboration, *Measurement of the Inclusive Charge Flow in Hadronic Z Decays,* DELPHI 96-19 PHYS 594.

[67] OPAL Collaboration, P. D. Acton *et al.*, Phys. Lett. **B294** (1992) 436.

[68] T. Sjöstrand, Comp. Phys. Comm. **82** (1994) 74.

[69] G. Marchesini *et al.*, Comp. Phys. Comm. **67** (1992) 465.

[70] SLD Collaboration, J. Brau, *Electroweak Precision Measurements with Leptons*, talk presented at EPS-HEP-99, Tampere, Finland, 15-21 July 1999.

[71] CHARM II Collaboration, P. Vilain *et al.*, Phys. Lett. **B335** (1994) 246.

[72] UA2 Collaboration, J. Alitti *et al.*, Phys. Lett. **B276** (1992) 354.

[73] CDF Collaboration, F. Abe *et al.*, Phys. Rev. Lett. **65** (1990) 2243;
CDF Collaboration, F. Abe *et al.*, Phys. Rev. **D43** (1991) 2070.

[74] CDF Collaboration, F. Abe *et al.*, Phys. Rev. Lett. **75** (1995) 11;
CDF Collaboration, F. Abe *et al.*, Phys. Rev. **D52** (1995) 4784.
A. Gordon, talk presented at XXXIInd Rencontres de Moriond, Les Arcs, 16-22 March 1997, to appear in the proceedings.

[75] DØ Collaboration, S. Abachi *et al.*, Phys. Rev. Lett. **84** (2000) 222.

[76] `http://www-cdf.fnal.gov/physics/ewk/wmass_new.htm`.

[77] CDF Collaboration, W. Yao, *t Mass at CDF*, talk presented at ICHEP 98, Vancouver, B.C., Canada, 23-29 July, 1998.

[78] DØ Collaboration, B. Abbott *et al.*, Phys. Rev. Lett. **84** (2000) 222.

[79] The Top Averaging Group, L. Demortier *et al.*, for the CDF and DØ Collaborations, FERMILAB-TM-2084 (1999).

[80] CCFR/NuTeV Collaboration, K. McFarland *et al.*, Eur. Phys. Jour. **C1** (1998) 509.

[81] NuTeV Collaboration, K. McFarland, talk presented at the XXXIIIth Rencontres de Moriond, Les Arcs, France, 15-21 March, 1998, hep-ex/9806013. The result quoted is a combination of the NuTeV and CCFR results.

[82] T. van Ritbergen and R.G. Stuart, Phys. Rev. Lett. **82** (1999) 488.

[83] H. Burkhardt and B. Pietrzyk, *Update of the hadronic contribution to the QED vacuum polarisation* Preprint LAPP-EXP 2001-03, accepted by Phys. Lett. **B**.

[84] *Reports of the working group on precision calculations for the Z resonance*, eds. D. Bardin, W. Hollik and G. Passarino, CERN Yellow Report 95-03, Geneva, 31 March 1995.

[85] G. Degrassi, S. Fanchiotti and A. Sirlin, Nucl. Phys. **B351** (1991) 49;
G. Degrassi and A. Sirlin, Nucl. Phys. **B352** (1991) 342;
G. Degrassi, P. Gambino and A. Vicini, Phys. Lett. **B383** (1996) 219;
G. Degrassi, P. Gambino and A. Sirlin, Phys. Lett. **B394** (1997) 188;
G. Degrassi and P. Gambino, Nucl. Phys. **B567** (2000) 3.

[86] A. Czarnecki and J. Kühn, Phys. Rev. Lett. **77** (1996) 3955;
R. Harlander, T. Seidensticker and M. Steinhauser, Phys. Lett. **B426** (1998) 125.

[87] Electroweak libraries:
ZFITTER: see Reference 37;
BHM (G. Burgers, W. Hollik and M. Martinez): W. Hollik, Fortschr. Phys. **38** (1990) 3, 165;
M. Consoli, W. Hollik and F. Jegerlehner: Proceedings of the Workshop on Z physics at LEP I, CERN Report 89-08 Vol.I,7 and G. Burgers, F. Jegerlehner, B. Kniehl and J. Kühn: the same proceedings, CERN Report 89-08 Vol.I, 55;
TOPAZ0 Version 4.0i: G. Montagna, O. Nicrosini, G. Passarino, F. Piccinni and R. Pittau, Nucl. Phys. **B401** (1993) 3; Comp. Phys. Comm. **76** (1993) 328.
These computer codes have upgraded by including the results of [84] and references therein. ZFITTER and TOPAZ0 have been further updated using the results of references 85 and 86. See, D. Bardin and G. Passarino, *Upgrading of Precision Calculations for Electroweak Observables*, CERN-TH/98-92, hep-ph/9803425.

[88] A. Freitas, W. Hollik, W. Walter and G. Weiglein, Phys. Lett. **B495** (2000) 338.

[89] T. Hebbeker, M. Martinez, G. Passarino and G. Quast, Phys. Lett. **B331** (1994) 165;
P.A. Raczka and A. Szymacha, Phys. Rev. **D54** (1996) 3073;
D.E. Soper and L.R. Surguladze, Phys. Rev. **D54** (1996) 4566.

[90] M. Steinhauser, Phys. Lett. **B429** (1998) 158.

[91] S. Eidelmann and F. Jegerlehner, Z. Phys. **C67** (1995) 585.

[92] The BES Collaboration, J.Z.Bai *et al.*, *Measurements of the Cross Section for $e^+e^- \to$ hadrons at Center-of-Mass Energies from 2 to 5 GeV*, hep-ex/0102003.

[93] M. L. Swartz, Phys. Rev. **D53** (1996) 5268.

[94] A.D. Martin and D. Zeppenfeld, Phys. Lett. **B345** (1994) 558.

[95] R. Alemany, *et al.*, Eur. Phys. J. **C2** (1998) 123.

[96] M. Davier and A. Höcker, Phys. Lett. **B419** (1998) 419.

[97] J.H. Kühn and M. Steinhauser, Phys. Lett. **B437** (1998) 425.

[98] J. Erler, Phys. Rev. **D59**, (1999) 054008.

[99] A. D. Martin, J. Outhwaite and M. G. Ryskin, Phys. Lett. **B492** (2000) 69.

[100] F. Jegerlehner, *Hadronic Effects in (g-2) and $\alpha_{QED}(M_Z)$: Status and Perspectives*, Proc. of Int. Symp. on Radiative Corrections, Barcelona, Sept. 1998, page 75.

[101] Particle Data Group (D.E. Groom *et al.*), Eur. Phys. J. **C15** (2000) 1.

[102] K.Hoffman, *Year 2000 update for OPAL and LEP HIGGSWG results"*, talk presented at ICHEP2000, Osaka, July 27 - August 2,2000, to appear in the proceedings.